



Politecnico di Torino

A.Y. 2024/2025

Master degree in Automotive Engineering

Propulsion System - Reports

Students:

Emanuele Landolina (S349706)
Marcello Marrella (S346927)
Giuseppe Martire (S344386)

Contents

Contents	i
List of Figures	ii
List of Tables	iii
1 Air fuel cycle and flywheel dimensioning	1
1.1 Introduction	1
1.2 Key-points of the a-f cycle	3
1.2.1 Analysis of the thermodynamic cycle	5
1.3 Calculation of imep	9
1.4 Single-cylinder engine calculations	10
1.4.1 Inertia pressure and effective pressure	10
1.4.2 Moment acting on the crankshaft	11
1.4.3 Calculation of the flywheel diameter	14
1.4.4 Instantaneous crankshaft speed	17
1.5 Multi-cylinder engine calculations	18
1.5.1 Moment acting on the crankshaft	18
1.5.2 Calculation of the flywheel diameter	20
1.5.3 Instantaneous crankshaft speed	21
2 Engine testing and HRR analysis	22
2.1 Engine testing	22
2.1.1 Steady state test	24
2.2 HRR analysis	31
2.2.1 Evaluation and filtering of in-cylinder pressure signal	31
2.2.2 Combustion diagnostic and mass fraction burned calculations	33

List of Figures

Figure 1.1	Exploded view of the crankshaft	1
Figure 1.2	A-f cycle on p-V diagram	8
Figure 1.3	In-cylinder pressure vs crank angle degrees	8
Figure 1.4	Effective pressure as a function of crank angle	11
Figure 1.5	A-f cycle with inertia pressure (properly over imposed)	11
Figure 1.6	Forces acting on the piston	12
Figure 1.7	Tangential pressure p_t as function of the crank angle	12
Figure 1.8	Normalized shaft and resistant work over a cycle + tangential and resistant pressure	14
Figure 1.9	Instantaneous crankshaft speed for single cylinder engine	18
Figure 1.10	Tangential pressure for multi-cylinder engine	19
Figure 1.11	Normalized shaft and resistant work over a cycle + tangential and resistant pressure	20
Figure 1.12	Instantaneous crankshaft speed for multi cylinder engine	21
Figure 2.1	Engine testbed	23
Figure 2.2	Correction factor	26
Figure 2.3	Mechanical characteristic	27
Figure 2.4	Brake specific fuel consumption	28
Figure 2.5	Brake specific fuel consumption	28
Figure 2.6	Fuel conversion efficiency	29
Figure 2.7	Fuel conversion efficiency	29
Figure 2.8	Volumetric efficiency	30
Figure 2.9	Average cycle as a pressure raw signal	32
Figure 2.10	Signal comparison after filtering	33
Figure 2.11	Comparison of cycles	34
Figure 2.12	HRR and injection current	34
Figure 2.13	SOI from injection current signal	35
Figure 2.14	SOC from Heat Release Rate	35
Figure 2.15	Mass fraction burned	36

List of Tables

Table 1.1	Fixed engine characteristics	3
Table 1.2	Computed engine characteristic	3
Table 1.3	Data for key points calculation	4
Table 1.4	Data for the calculation of the lower heating value at T_2	4
Table 1.5	Key points values	7
Table 1.6	Data for flywheel design	14
Table 1.7	Schematic computation of ΔW	15
Table 2.1	Engine characteristics	22
Table 2.2	Reference conditions and properties of air, fuel and EGR	23
Table 2.3	Test results	24
Table 2.4	Test results	24
Table 2.5	ISO1585 Calculations	26
Table 2.6	Volumetric efficiency	30

Report 1

Air fuel cycle and flywheel dimensioning

1.1 Introduction

The aim of this study is to design a flywheel in order to stabilize the crankshaft speed, minimizing wide speed oscillations without compromising engine torque or power.

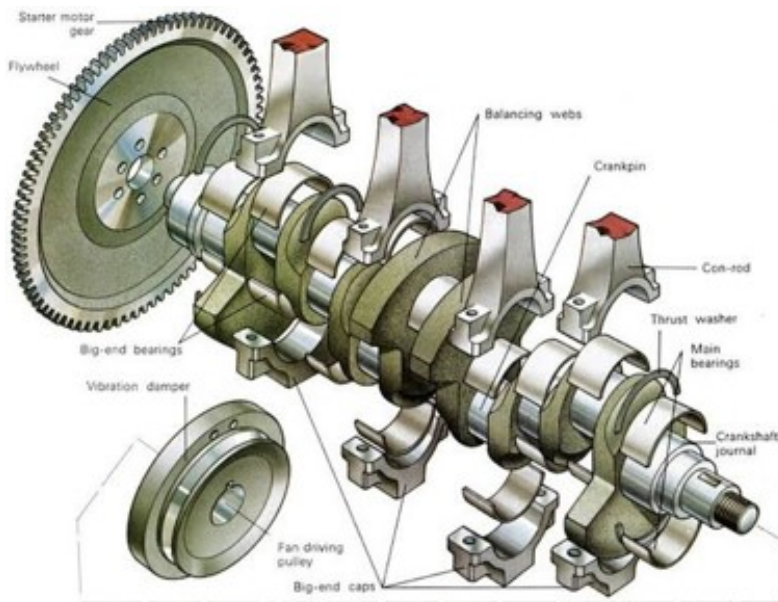


Figure 1.1: Exploded view of the crankshaft

$$M_{shaft}(\theta) - M_{load} = J \cdot \frac{d\omega}{dt} \quad (1.1)$$

$$J = J_{eng} + J_{flywheel} \quad (1.2)$$

In equation 1.1 the turning moments M_{shaft} and M_{load} are related to inertia moment J and angular acceleration $\frac{dw}{dt}$. Since wide speed oscillations must be avoided (i.e $\frac{dw}{dt}$ should be kept as low as possible) a proper design of the flywheel is desired, in order to achieve higher inertia moment. The design depends on forces acting on the piston and the consequent turning moment acting on the crankshaft: these are going to be evaluated for an SI naturally aspirated engine (with port fuel injection) starting from a steady-state operating point at full load.

An air-fuel (a-f) cycle with some modifications is considered:

- intake and exhaust valves instantaneously open/closed at dead centers.
- Compression phase ($1 \rightarrow 2$) and expansion phase ($3 \rightarrow 4$) are described as polytrophic transformations, with m and m' as polytrophic indexes.
- Combustion phase ($2 \rightarrow 3$) and blowdown phase ($4 \rightarrow 5$) occur at constant volume. Combustion is diabatic since heat transfer occurs.
- Intake phase ($7 \rightarrow 1$) and exhaust phase ($5 \rightarrow 6$) occur at constant pressure.
- Blow off ($6 \rightarrow 7$) is considered: part of the residual gas leaves the combustion chamber, causing an instantaneous decrement of pressure inside the chamber; this does not affect $p_{im}(= p_a)$. The condition $p_a > p_7$ is what ensures the natural motion of charge inside the cylinder (beginning of intake phase).
- No leakages.
- Specific heats c_p and c'_p are assumed different but independent from temperature.

1.2 Key-points of the a-f cycle

In order to evaluate forces acting on the piston and the consequent turning moment acting on the crankshaft, an analysis of the thermodynamic state of the closed system (composed by air, fuel and residual gas) is firstly accomplished.

Parameter	Value	Unit
Number of cylinders (i)	4	-
Bore (B)	95.8	mm
Stroke (S)	78.95	mm
Compression ratio (r_c)	11	-
Crank slider parameter (Λ)	0.306	-
Engine speed (n)	6000	rpm
Reciprocating masses (m_{rec}/V_d)	1.2	kg/dm ³
Equivalent rotating masses (m_{rot}/V_d)	0.85	kg/dm ³

Table 1.1: Fixed engine characteristics

Knowing the engine characteristic illustrated in table 1.1, it is possible to compute other geometrical parameters:

- displacement volume

$$V_d = \pi \cdot \frac{B^2}{4} \cdot S$$

- clearance volume

$$V_c = V_d \cdot \left(\frac{1}{r_c - 1} \right)$$

- total volume

$$V_t = V_d + V_c$$

The values are shown in table 1.2.

Parameter	Value	Unit
Displacement volume (V_d)	310820	mm ³
Clearance volume (V_c)	31082	mm ³
Total volume (V_t)	341902	mm ³

Table 1.2: Computed engine characteristic

Starting from the knowledge of some engine characteristic values (table 1.1 and table

1.2) and from several fixed data for each point calculation (table 1.3 and table 1.4) the key points of the thermodynamic cycle can be computed.

Point	Parameter	Value	Unit
Point 1	Environmental pressure (p_a)	100	kPa
	Environmental temperature (T_a)	293	K
	Volumetric efficiency ($\lambda_v = m_a/m_{a,id}$)	0.82	—
	Residual to environmental pressure ratio (p_r/p_a)	1.15	—
	Residual temperature (T_r)	900	K
	Stoichiometric air to fuel ratio ($\alpha_{st} = (m_a/m_f)_{st}$)	14.7	—
	Relative air to fuel ratio (α/α_{st})	0.95	—
	Fuel specific heat (c_f)	2500	J/(kg · K)
	Fuel vaporized fraction ($x = m_{f(vap)}/m_{f(liq)}$)	1	—
	Fuel vaporization heat (r)	320000	J/kg
	ΔT for the air-fuel-residual mixture during the intake	30	°C
	Air elastic constant (R)	287.2	J/(kg · K)
	Burnt gas elastic constant (R')	288	J/(kg · K)
Point 2	Air-fuel-residual mixture elastic constant ($R1$)	271	J/(kg · K)
	Air specific heat (c_p)	1009	J/(kg · K)
Point 3	Burnt gas specific heat (c'_p)	1150	J/(kg · K)
	Compression index (m)	1.35	—
	Dissociation heat ($\Delta Q_d = d_q \cdot (T_3 - T_d)^2$)		kJ/kg
	d_q	0.54	J/(kg · K ²)
Point 3	T_d	1850	K
	Burnt gas elastic constant (R')	288	J/(kg · K)
	Burnt gas specific heat (c'_p)	1328	J/(kg · K)
	Burnt gas specific heat (c'_v)	1040	J/(kg · K)
Point 4	Heat losses coefficient (δA)	0.06	—
	Expansion index (m)	1.27	—

Table 1.3: Data for key points calculation

Parameter	Value	Unit
Air specific heat (c_v)	744	J/(kg · K)
Burnt gas specific heat (c'_v)	824	J/(kg · K)
Lower heating value at $T_0 = 288K$ ($Q_{LHV}(T_0)$)	44000	kJ/kg

Table 1.4: Data for the calculation of the lower heating value at T_2

1.2.1 Analysis of the thermodynamic cycle

Point 1: application of the 1st principle of Thermodynamics in the Lagrangian form (closed system) to the transformation $6 \rightarrow 1$.

$$Q = W + \Delta U^* + \underbrace{\Delta E_{k,g,\dots}}_{\approx 0} \quad (1.3)$$

Control mass: $m_1 = m_a + m_f + m_r$

For the calculations of Point 1, the following considerations have been made:

- The variation of the chemical internal energy is zero since no chemical reaction occurs during the process:

$$U^* = \underbrace{U_t}_{\propto c_v T} + \underbrace{U_{ch}}_{=0} \quad (1.4)$$

- The work done by the system through the control surface is the sum of:
 - work done by the piston;
 - work (negative) done by the external environment to *push* inside the cylinder the volume of air and fuel.

$$W = \int_6^1 p \cdot dV = \int_{6_{ext}}^1 p \cdot dV + \int_{6_{piston}}^1 p \cdot dV \quad (1.5)$$

- The temperature of the air, the fuel and residuals mixture is increased by $30 \text{ } ^\circ\text{C}$ due to the heat exchanged during the process.

These considerations lead to the following equations:

$$T_1 = \Delta T + \frac{c_{p,a} \cdot T_a \cdot \alpha + \alpha' \cdot c_{p'} \cdot T_r + c_f \cdot T_f - x \cdot r}{c_f + \alpha \cdot c_{p,a} + \alpha' \cdot c_{p'}} \quad (1.6)$$

$$p_1 = p_a \left[\lambda_v \cdot (r_c - 1) \cdot \frac{\alpha + 1}{\alpha} \cdot \frac{1}{RT_a} + \frac{p_r}{p_a} \cdot \frac{1}{R'T_r} \right] \frac{R_1 T_1}{r_c} \quad (1.7)$$

Point 2: the real transformation can be approximated by means of a polytropic one (neglecting leakages) $pV^m = \text{const}$, provided that its final point (2^{pol}) corresponds to the real final point (2) by properly choosing the polytropic exponent m . The transformation cannot be considered isentropic due to heat exchanged from the cylinder walls to the gas and vice versa ($m \neq \gamma = c_p/c_v$).

The entropy decreases from point 1 to point 2 ($ds < 0$): this can be seen from the second law of thermodynamics and the relations of heat and specific heat:

$$T \cdot ds = \delta Q + \delta L_w \quad (1.8)$$

$$\delta Q < 0 \iff c \cdot (T_2 - T_1) < 0 \implies c < 0 \implies c_v \cdot \frac{m - \gamma}{m - 1} < 0 \quad \text{with } 1 < m < \gamma$$

These relations lead to the following equations:

$$\begin{cases} T_2 = T_1 \cdot r_c^{m-1} \\ p_2 = p_1 \cdot r_c^m \end{cases} \quad (1.9)$$

Point 3: application of the first principle of Thermodynamics in the Lagrangian form (closed system) to the transformation $2 \rightarrow 3$ (constant volume combustion with heat transfer).

For the calculations of Point 3, a real combustion is taken into account, involving the following hypothesis:

- the presence of residuals (α');
- dissociation for $T > T^* = 1850K$;
- heat transfer by means of a “reduction” coefficient $(1 - \delta_A)$ of the heat given by combustion to the burned gases;
- fuel-rich mixture: the stoichiometric fuel mass burns, while the excess fuel acts as inert.

To compute the gas temperature at the end of combustion, we start from the definition of Lower Heating Value (LHV):

$$Q_{LHV,v}(T_2) = Q_{LHV,v}(T_0) + (c_v - c'_v)(T_2 - T_0)(\alpha + 1) \quad (1.10)$$

where $Q_{LHV,v}(T_2)$ is the amount of heat that must be exchanged to return to T_2 .

Once $Q_{LHV,v}(T_2)$ is evaluated, it is possible to calculate T_3 using the equation 1.11.

$$\underbrace{d_q}_{a} T_3^2 + \underbrace{(\bar{c}'_v - 2T^* d_q)}_{b} T_3 + \underbrace{\left(-\bar{c}'_v T_2 + d_q(T^*)^2 - (1 - \delta_A) \cdot \frac{\alpha}{\alpha_{st}} \cdot \frac{Q_{LHV,v}(T_2)}{1 + \alpha + \alpha'} \right)}_{c} = 0 \quad (1.11)$$

$$aT_3^2 + bT_3 + c = 0 \implies T_3 \begin{cases} \nearrow > 1850^\circ K \\ \searrow \text{not meaningful} \end{cases}$$

Now it is possible to write the gas law for points 2 and 3 knowing T_2 and p_2 (from equations 1.9) knowing T_3 (from equation 1.11):

$$\begin{cases} p_2 V_2 = M_2 R_2 T_2 \\ p_3 V_3 = M_3 R_3 T_3 \end{cases} \quad (1.12)$$

Starting from equation 1.12, the condition $M_2 = M_3$ and $V_2 = V_3$ are taken into account, and therefore p_3 can be computed using the equation 1.13.

$$p_3 = \frac{R'}{R_1} \cdot \frac{T_3}{T_2} \cdot p_2 \quad (1.13)$$

Point 4: we can consider a polytrophic transformation (neglecting leakages) $pV^{m'} = const$, choosing m' so that the final point of this polytrophic transformation coincides with the final point of the real transformation. In this case, in-cylinder gas is always hotter than the cylinder walls, therefore the heat flux only occurs in one direction.

$$\begin{cases} p_4 = p_3 \cdot r_c^{1-m'} \\ T_4 = T_3 \cdot r_c^{1-m'} \end{cases} \quad (1.14)$$

Key point	p [bar]	T [K]	V [mm^3]
1	0.89	330.15	V_t
2	22.54	764.18	V_c
3	85.93	2740.88	V_c
4	4.09	1434.55	V_t

Table 1.5: Key points values

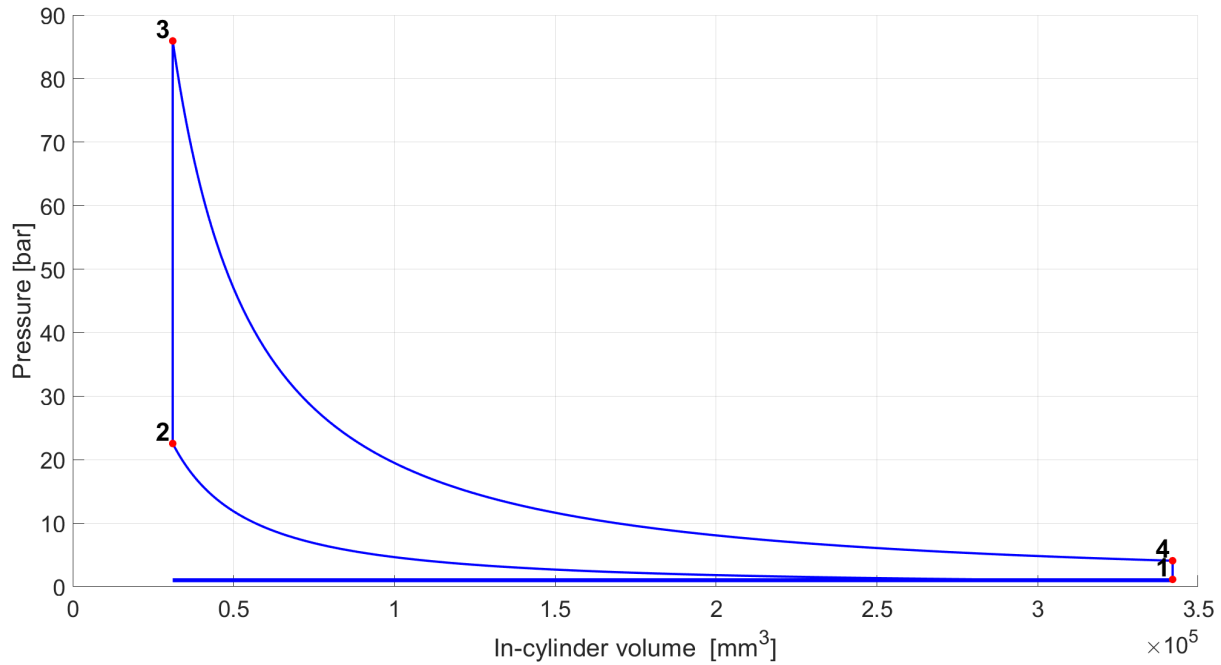


Figure 1.2: A-f cycle on p-V diagram

Plotting the gas pressure over an entire cycle (from 0° to 720°) there are some points where the function is not continuous; due to the assumption that combustion ($2 \rightarrow 3$), blow-down ($4 \rightarrow 5$) and blow-off phenomena ($6 \rightarrow 7$) occur at constant in-cylinder volume, for $\theta = 180^\circ, 360^\circ$ and 720° (or 0°) it is possible to observe that jump points are present.

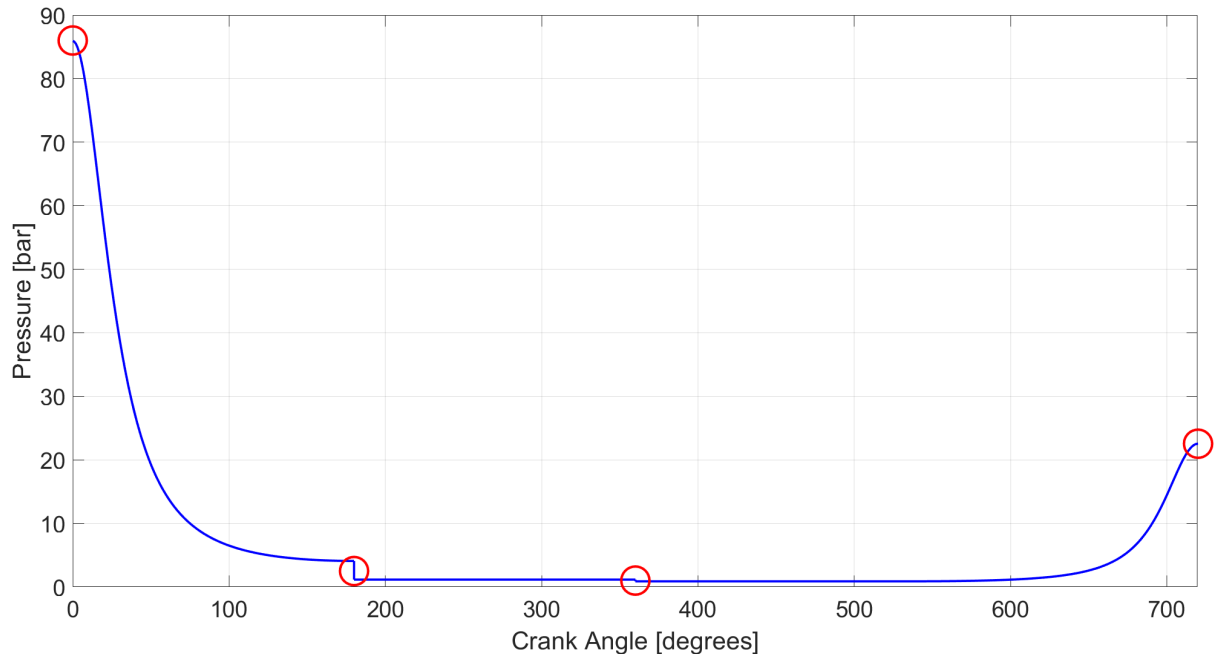


Figure 1.3: In-cylinder pressure vs crank angle degrees

1.3 Calculation of imep

The indicated mean effective pressure can be evaluated as the ratio of the indicated work of the piston (computed over the thermodynamic cycle) and his displacement between the dead centers.

$$imep = \frac{W}{V_d} = \frac{\oint p dV}{V_d} = \frac{1}{V_d} \left[\int_1^2 p dV + \cancel{\int_2^3 p dV} + \int_3^4 p dV + \right. \\ \left. + \cancel{\int_4^5 p dV} + \int_5^6 p dV + \cancel{\int_6^7 p dV} + \int_7^1 p dV \right] \quad (1.15)$$

Since combustion ($2 \rightarrow 3$), blow-down ($4 \rightarrow 5$) and blow-off phenomena ($6 \rightarrow 7$) occur at constant in-cylinder volume, the indicated work related to these transformation is null. Manipulating the integral terms of the previous equation, imep can be algebraically computed as it follows:

$$imep = p_1 \cdot \frac{r_c}{r_c - 1} \cdot \frac{1}{1-m} (r_c^{m-1} - 1) + p_3 \cdot \frac{1}{r_c - 1} \cdot \frac{1}{1-m'} (r_c^{1-m'} - 1) + (p_1 - p_r) \quad (1.16)$$

Alternatively, *imep* can also be analytically computed using the Matlab function trapz() to evaluate the integral of the pressure over each transformation of the cycle.

MATLAB script - imep calculation

```

1 W34 = trapz(Vx(1:181), p_gas34(1:181));
2 W56 = trapz(Vx(181:361), p_gas56(181:361));
3 W71 = trapz(Vx(361:541), p_gas71(361:541));
4 W12 = trapz(Vx(541:721), p_gas12(541:721));
5 imep = (W34 + W56 + W71 + W12)/Vd;

```

Both methods provide the same result of $imep = 11.25 \text{ bar}$.

1.4 Single-cylinder engine calculations

1.4.1 Inertia pressure and effective pressure

The acceleration of the piston can be evaluated using the equation 1.17.

$$a_p = \ddot{x} = \omega^2 r \cdot \left(\cos \theta + \Lambda \cdot \frac{\cos 2\theta}{\cos \beta} \right) \quad (1.17)$$

$$F_i = -m_{rec} \cdot a_p = -m_{rec} \cdot \omega^2 r \cdot \left(\cos \theta + \Lambda \cdot \frac{\cos 2\theta}{\cos \beta} \right) \quad (1.18)$$

where $\omega = \omega_{avg} = n \cdot \frac{2\pi}{60}$ in rad/s and $r = \frac{S}{2}$ is the crank length in meters.

The inertia pressure can be also expressed considering the mean piston speed $u = 2Sn$:

$$p_i = \frac{F_i}{A_p} = - \left(\frac{m_{rec}}{V_d} \right) \cdot \frac{\pi^2 u^2}{2} \cdot \left(\cos \theta + \Lambda \cdot \frac{\cos 2\theta}{\cos \beta} \right) \quad (1.19)$$

Since $[F_i] = N$ and $[A_p] = mm^3$, the inertia pressure is computed in MPa. As a consequence, a factor of 10 must be applied in order to get a proper comparison of all the pressure acting on the piston expressed in bar.

In order to evaluate the effective pressure acting on the piston and the connecting rod, different contributes must be considered:

$$p_{eff} = p_{gas} - p_c \pm p_i \quad (1.20)$$

Since the in-cylinder gas pressure p_{gas} over the entire cycle has been previously plotted in figure 1.2 and the crankcase pressure is assumed constant ($p_c \simeq 1$ bar), if the inertia pressure p_i is known then also the effective pressure p_{eff} can be easily computed.

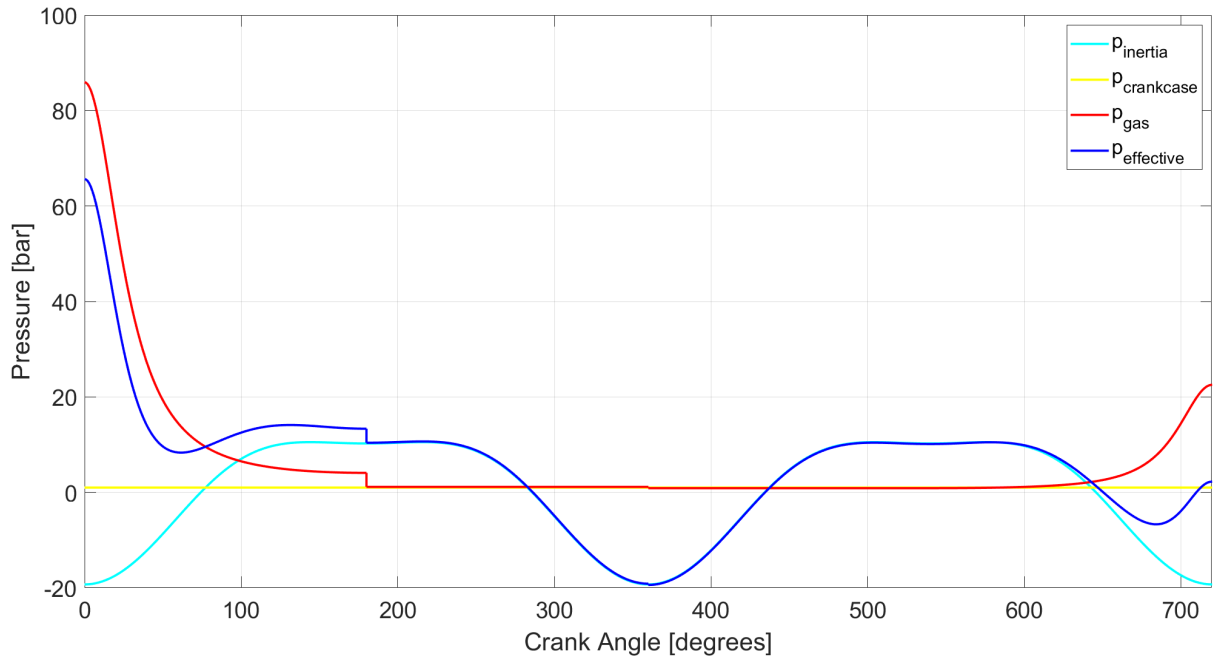


Figure 1.4: Effective pressure as a function of crank angle

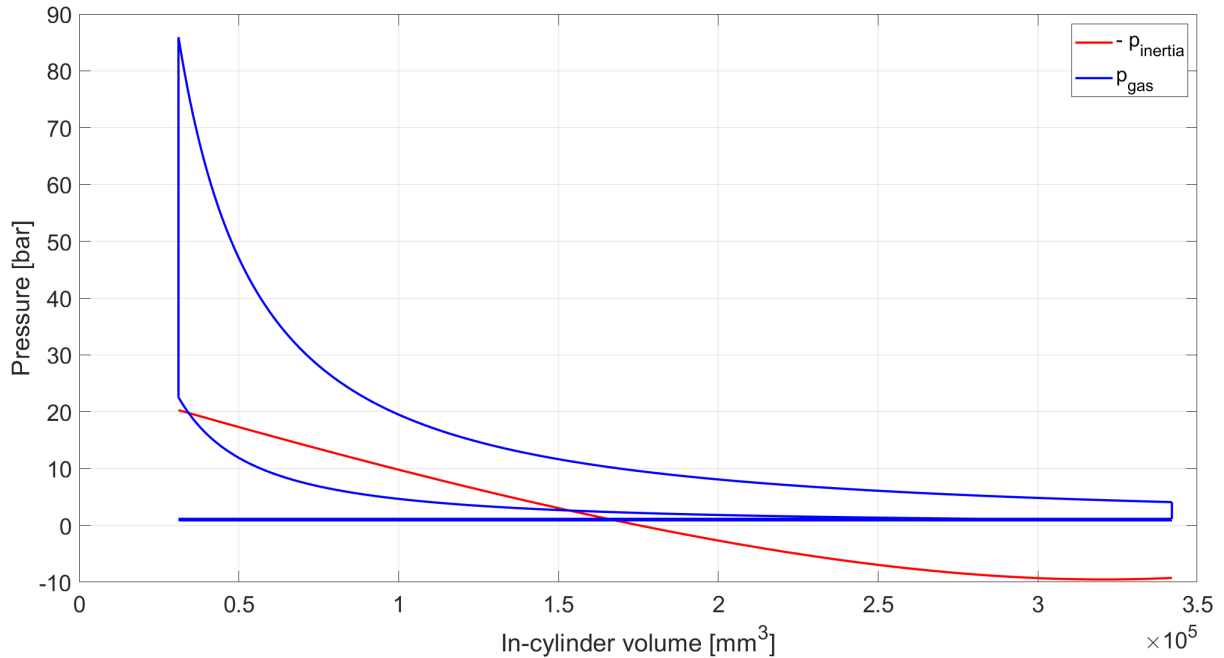


Figure 1.5: A-f cycle with inertia pressure (properly over imposed)

The inertia pressure (red curve in figure 1.5) has a period corresponding to half the engine cycle and it is plotted placing the 0 of the y – axis at ambient pressure.

1.4.2 Moment acting on the crankshaft

Through a decomposition of forces, the effective pressure $p_{eff}(\theta)$ and his consequent force $P(\theta)$ acting on the piston are relatable to a tangential pressure $p_t(\theta)$ and his con-

sequent force $F_T(\theta)$. This tangential contribute determines the shaft moment acting on the crankshaft (the one already mentioned in equation 1.1).

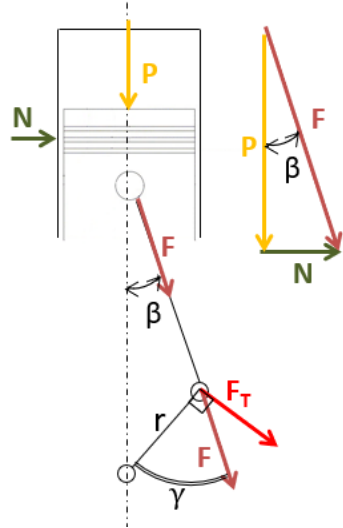


Figure 1.6: Forces acting on the piston

$$M_s(\theta) = F_T \cdot r = p_{eff} \cdot \frac{V_d}{2} \cdot \frac{\sin(\beta + \theta)}{\cos \beta}$$

$$p_t(\theta) = \frac{M_s(\theta)}{\frac{V_d}{2}} = p_{eff} \cdot \frac{\sin(\beta + \theta)}{\cos \beta}$$

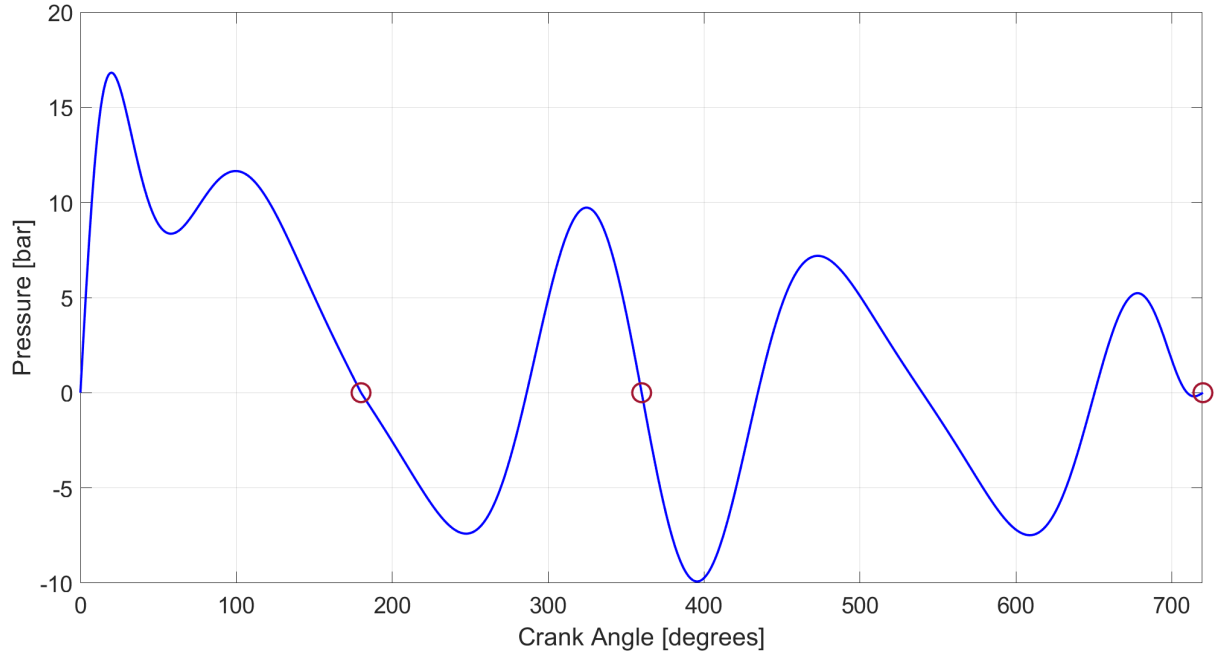


Figure 1.7: Tangential pressure p_t as function of the crank angle

The tangential pressure (and the shaft moment) is zero at DC positions (as $\theta = 0^\circ$ or

$\theta = 180^\circ$). Moreover, discontinuities in the slope of p_t around DCs (except $\theta = 540^\circ$) are expected due to discontinuities previously noted in p_{eff} .

Mathematical explanation:

$$\left. \frac{dp_t}{d\theta} \right|_{DC} = \frac{d}{d\theta} \left(p_{eff} \cdot \underbrace{f(\theta)}_{\frac{\sin \beta + \theta}{\cos \beta}} \right) = p_{eff} \cdot \frac{df(\theta)}{d\theta} + f(\theta) \cdot \cancel{\frac{dp_{eff}}{d\theta}}$$

0 @ DC

$$\frac{dp_{eff}}{d\theta} = \frac{dp_{eff}}{dx} \cdot \underbrace{\frac{dx}{dt}}_{\dot{x}} \cdot \underbrace{\frac{dt}{d\theta}}_{\frac{1}{\omega}} \implies \frac{dp_{eff}}{d\theta} = 0 \text{ because at DC velocity } \dot{x} \text{ is zero instantaneously}$$

Moreover, since we are considering a steady-state condition, the instantaneous rotational speed of the engine at the beginning of the cycle is equal to the speed at the end of the cycle: $\omega(0) = \omega(4\pi)$.

Integrating the previous equation, it is possible to calculate the resistant moment which can be considered constant over an engine cycle.

Calculations $M_r(\theta) \rightarrow p_r(\theta)$:

$$\int_0^{4\pi} M_s(\theta) d\theta - \int_0^{4\pi} M_r(\theta) d\theta = \int_0^{4\pi} J \frac{d\omega}{dt} d\theta$$

steady state condition:

$$W_s - W_r = \int_{\omega(0)}^{\omega(4\pi)} J \cdot \omega d\omega = 0$$

This means that resistant work, moment and pressure can be computed as follow:

$$\begin{aligned} W_s &= W_r = imep \cdot V_d = 349.59J \\ M_r &= \frac{W_r}{4\pi} = \frac{imep \cdot V_d}{4\pi} = 27.82Nm \\ p_r &= \frac{M_r}{\frac{V_d}{2}} = \frac{F_r}{A_p} \cdot \frac{r}{\frac{S}{2}} = \frac{\frac{imep \cdot V_d}{4\pi}}{\frac{V_d}{2}} = \frac{imep}{2\pi} = 1.79bar \end{aligned}$$

Normalizing the shaft and resistant work with respect to the unitary displacement, it is possible to plot these quantities together with the tangential and resistant torque (apart from a scaling factor, the two “work” terms are the integral of the two pressures).

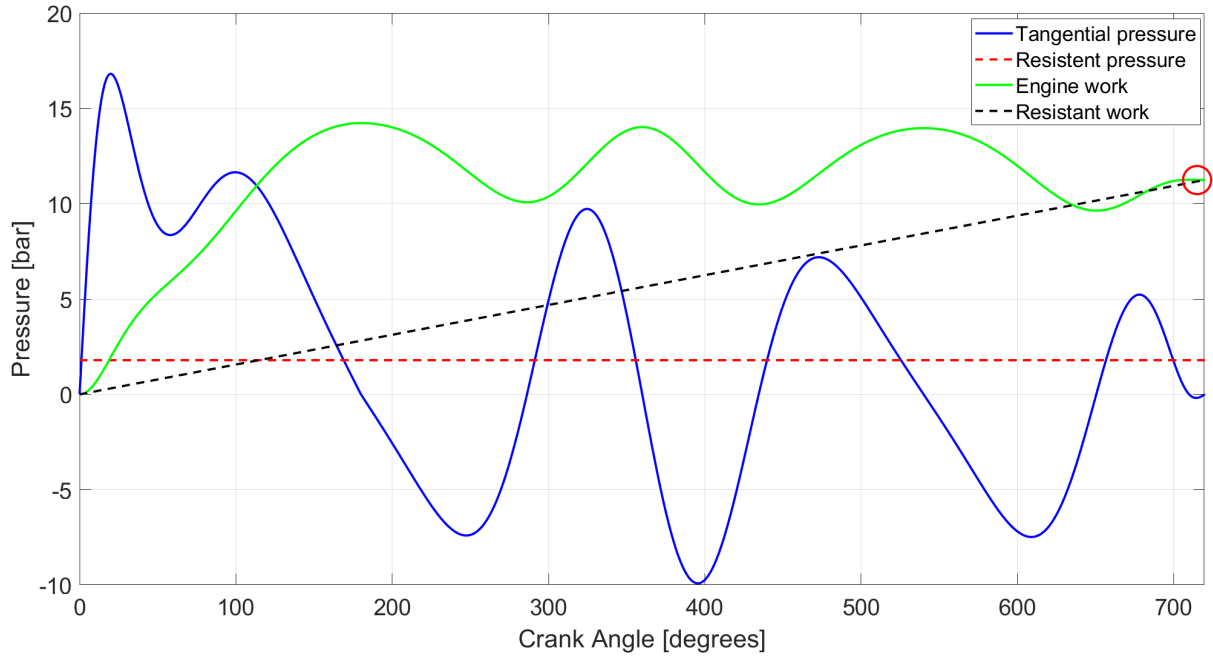


Figure 1.8: Normalized shaft and resistant work over a cycle + tangential and resistant pressure

From figure 1.8 it is verified that shaft work and resistant work are equal at the end of the cycle.

1.4.3 Calculation of the flywheel diameter

For the dimensioning of the flywheel, the engine is assumed disconnected from the transmission and therefore only engine inertia J_{eng} and flywheel inertia J_{flyw} are taken into account to evaluate the total inertia J :

$$J = J_{eng} + J_{flyw} \quad (1.21)$$

Parameter	Value	Unit
Metal density (ρ)	7700	kg/m^3
Cinematic irregularity (δ)	0.01	-

Table 1.6: Data for flywheel design

In order to set a limit to the maximum allowed speed fluctuation, a *kinematic irregularity target* (equation 1.22) is defined and fixed to 1%.

$$\delta = \frac{\omega_{max} - \omega_{min}}{\omega_{avg}} = 1\% = 0.01 \quad (1.22)$$

For the dimensioning, the *dynamic irregularity* coefficient (equation 1.23) must be evaluated.

$$\xi = \frac{\Delta W_{max} + |\Delta W_{min}|}{W \cdot 4\pi} = \frac{\Delta W_{tot}}{imep \cdot V_d} \quad (1.23)$$

The ΔW_{max} and ΔW_{min} are, respectively, the differences between the shaft work and the resistant work at the maximum and minimum instantaneous crankshaft speed $\omega(\theta)$. Their expressions as a function of the crankshaft are obtained integrating the equation of the shaft dynamic equilibrium between $\theta = 0$ and the angle which correspond to the maximum and to the minimum speed, $\theta(\omega_{max})$ and $\theta(\omega_{min})$, respectively.

Looking at table 1.7, ΔW_{max} and ΔW_{min} can be evaluated as the maximum and minimum values of $\Delta W(\theta)$ column.

θ	$W_s(\theta)$	$W_r(\theta)$	$\Delta W(\theta)$
0	$\int_0^0 M_s(\theta) d\theta = 0$	$\int_0^0 M_r(\theta) d\theta = 0$	$W_s(\theta) - W_r(\theta)$
1	$\int_0^1 M_s(\theta) d\theta$	$\int_0^1 M_r(\theta) d\theta$...
2	$\int_0^2 M_s(\theta) d\theta$	$\int_0^2 M_r(\theta) d\theta$...
:
720	$\int_0^{4\pi} M_s(\theta) d\theta = W_s$	$\int_0^{4\pi} M_r(\theta) d\theta = W_r$...

Table 1.7: Schematic computation of ΔW

$$\begin{cases} \Delta W_{max} = 357.55 \text{ J} \\ \Delta W_{min} = -17.74 \text{ J} \end{cases} \implies \Delta W_{tot} = \Delta W_{max} - \Delta W_{min} = 375.29 \text{ J} \quad (1.24)$$

Therefore, using the value of ΔW_{tot} evaluated in the equation 1.24, the value of ξ has been computed:

$$\xi = \frac{\Delta W_{tot}}{imep \cdot V_d} = 1.0735$$

As a consequence, it is possible to describe the dynamic irregularity as a function of the global rotating inertia J .

$$\begin{cases} \Delta W_{max} = \int_0^{\theta(\omega_{max})} J \cdot \frac{d\omega}{dt} d\theta = \int_{\omega(0)}^{\omega_{max}} J \cdot \omega d\omega = J \cdot \frac{\omega_{max}^2 - \omega_{(0)}^2}{2}, \\ \Delta W_{min} = \int_0^{\theta(\omega_{min})} J \cdot \frac{d\omega}{dt} d\theta = \int_{\omega(0)}^{\omega_{min}} J \cdot \omega d\omega = J \cdot \frac{\omega_{min}^2 - \omega_{(0)}^2}{2}. \end{cases}$$

Now, it is easy to calculate ΔW_{tot} as a difference of the two terms ΔW_{max} and ΔW_{min} :

$$\begin{aligned}\Delta W_{tot} &= \Delta W_{max} - \Delta W_{min} = J \cdot \left[\frac{\omega_{max}^2 - \omega_{(0)}^2}{2} - \frac{\omega_{min}^2 - \omega_{(0)}^2}{2} \right] = J \cdot \frac{\omega_{max}^2 - \omega_{min}^2}{2} = \\ &= J \cdot \frac{(\omega_{max} + \omega_{min})(\omega_{max} - \omega_{min})}{2} = J \cdot \omega_{avg} \cdot \delta\omega_{avg} = J \cdot \delta \cdot \omega_{avg}^2\end{aligned}\quad (1.25)$$

Using the equation of the dynamic irregularity 1.23 and the equation 1.25 just described, it is possible to compute the value of the inertia J :

$$\Delta W_{tot} = J \cdot \delta \cdot \omega_{avg}^2 = \xi \cdot imep \cdot V_d \implies J = \frac{\xi \cdot imep \cdot V_d}{\delta \cdot \omega_{avg}^2} = 0.0951 \text{ kg} \cdot \text{m}^2$$

According to the equation 1.21, the two main terms that are contributing to the value of J are expressed as it follows:

$$J_{eng} = \left(\frac{m_{rot}}{i V_d} \right) V_d \cdot r^2 = 1.03 \cdot 10^{-4} \text{ kg} \cdot \text{m}^2 \quad (1.26)$$

$$J_{flyw} = J - J_{eng} = 0.0950 \text{ kg} \cdot \text{m}^2 \quad (1.27)$$

Since J_{flyw} is known, the flywheel diameter can be determined as a consequence

$$\begin{aligned}J_{flyw} &= \int_{mass} r^2 \cdot dm = \int_{mass} r^2 \cdot \underbrace{2\pi r \cdot dr \cdot w_{flyw}}_{dV} \cdot \rho = 2\pi\rho \cdot w_{flyw} \cdot \int_0^{\frac{D}{2}} r^3 \cdot dr = \\ &= 2\pi\rho \cdot w_{flyw} \cdot \frac{r^4}{4} = \frac{\pi}{32}\rho \cdot w_{flyw} \cdot D^4\end{aligned}\quad (1.28)$$

where w_{flyw} is the width of the flywheel and D is the desired output of our dimensioning. Since also w_{flyw} is unknown, some constraints are going to be fixed in order to get a coherent dimensioning.

Supposing $w_{flyw} = \frac{1}{10}D$, it is possible to calculate the required flywheel diameter that allows to obtain the desired kinematic irregularity at the considered working point. The calculated diameter should stay within the range $2S < D < 5S$. If this condition is not verified:

- if $D > 5S$, it is possible to change the flywheel section (i.e. "C" shaped section instead of a planar disk);
- if $D < 2S$, then we should reduce the flywheel width (repeat the calculation of the diameter supposing $w_{flyw} = \frac{1}{15}D$).

Using the assumption just described and put it into the equation 1.28 and using the value in table 1.6 it is possible to compute the flywheel diameter D using the equation 1.29.

$$J_{flyw} = \frac{\pi}{32} \rho \cdot \frac{1}{10} D \cdot D^4 \implies D = \sqrt[5]{\frac{320 \cdot J_{flyw}}{\rho \cdot \pi}} = 0.2629 \text{ m} \quad (1.29)$$

It is possible to notice that for our calculation the condition $2S < D < 5S$ has been respected ($2S = 0.1579 \text{ m}$ and $5S = 0.3947 \text{ m}$) so there is no need to change the geometry.

As previously stated: $w_{flyw} = \frac{1}{10} D = 0.0263 \text{ m}$

1.4.4 Instantaneous crankshaft speed

Integrating the shaft dynamic equilibrium (equation 1.1) between $\theta = 0$ and generic crank angle θ it is possible to obtain an expression of the angular velocity $\omega(\theta)$.

$$\int_0^\theta M_s(\theta) d\theta - \int_0^\theta M_r(\theta) d\theta = \int_0^\theta J \frac{d\omega}{dt} d\theta \implies W_s(\theta) - W_r(\theta) = J \cdot \frac{\omega^2(\theta) - \omega_0(\theta)}{2}$$

$$\omega(\theta) = \sqrt{\omega_0^2 + \frac{2}{J} \cdot [W_s(\theta) - W_r(\theta)]} \quad (1.30)$$

In the equation 1.30, as a first approximation, $\omega(0) = \omega_{avg}$ is going to be considered to calculate a first attempt crankshaft speed:

$$\omega_I(\theta) = \sqrt{\omega_{avg}^2 + \frac{2}{J} \cdot [W_s(\theta) - W_r(\theta)]}$$

The estimation can be improved by iterating the process once the integral average of the previous estimation is computed:

$$\omega_{I,avg} = \langle \omega_I(\theta) \rangle$$

Therefore, a shift is going to be applied:

$$s = \omega_{I,avg} - \omega_{avg}$$

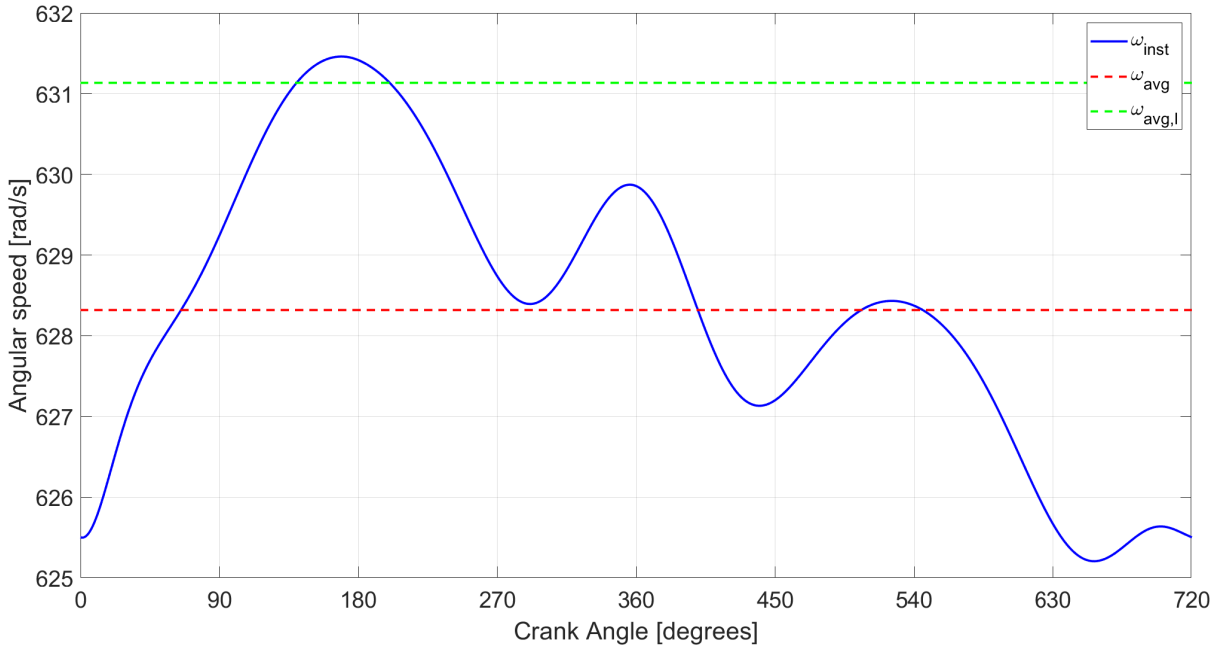


Figure 1.9: Instantaneous crankshaft speed for single cylinder engine

In this way, the average of the instantaneous crankshaft speed is the red fixed line, in figure 1.9, instead of the first iteration green one.

1.5 Multi-cylinder engine calculations

1.5.1 Moment acting on the crankshaft

In order to evaluate the total moment acting on the crankshaft in a multi cylinder engine, we need to sum up the contributions provided by each cylinder, considering the phase shift among them (equation 1.31, where m is the number of revs/cycle and i is the number of cylinders) and the firing order (1 – 3 – 4 – 2 for a four cylinders engine).

$$\Delta\varphi = \frac{m \cdot 360}{i} = 180 \quad (1.31)$$

Therefore the shaft moment can be evaluated with the equation 1.32.

$$M_{s, \text{multi-cyl}}(\theta) = \sum_{j=1}^i M_{s,j}(\theta - \varphi_j) \quad (1.32)$$

where $\varphi_j = (j - 1) \cdot \Delta\varphi$. Lastly, the tangential pressure plotted in figure 1.10 has been computed using the equation 1.33.

$$p_{t, \text{multi-cyl}}(\theta) = \frac{M_{s, \text{multi-cyl}}(\theta)}{\frac{V_d}{2}} \quad (1.33)$$

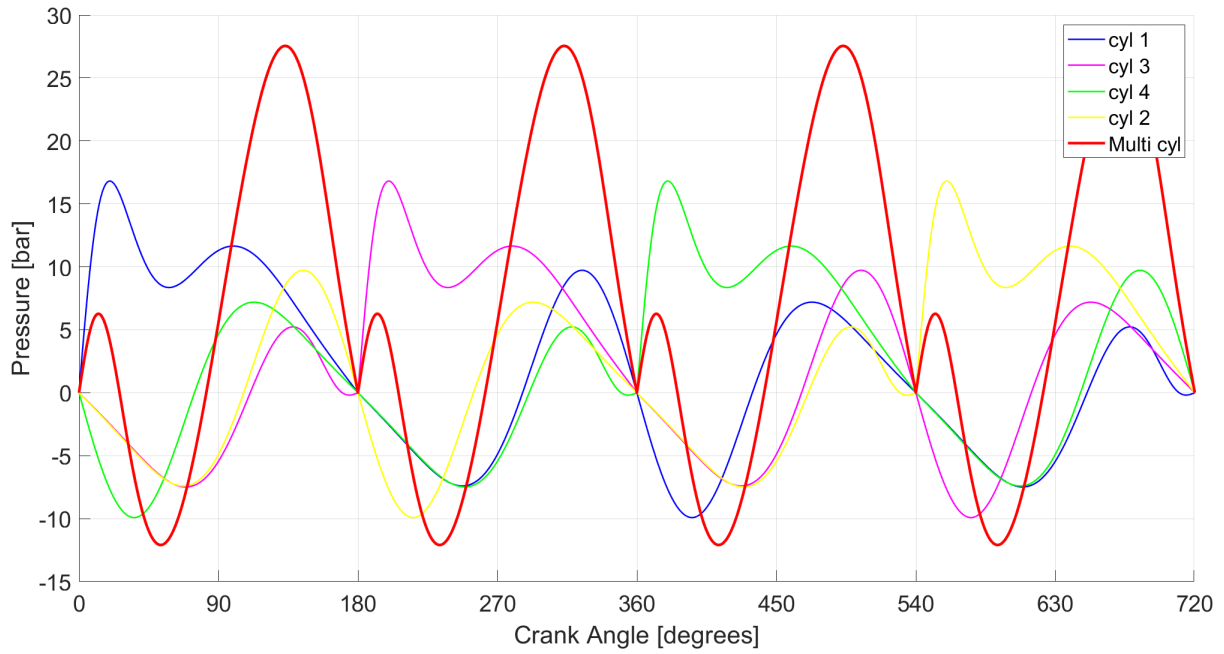


Figure 1.10: Tangential pressure for multi-cylinder engine

The shaft dynamic equilibrium has the following form:

$$M_{s, \text{multi-cyl}}(\theta) - M_{r, \text{multi-cyl}}(\theta) = J \cdot \frac{d^2\theta}{dt^2} = J \cdot \frac{d\omega}{dt} \quad (1.34)$$

Integrating the previous equation over the complete engine cycle (4π), we can obtain the resistant moment acting on the shaft. It is worthwhile to underline that the shaft moment integrated over the engine cycle is, by definition, the indicated work and that in this case this work is done by all the cylinders, therefore:

$$W_{r, \text{multi-cyl}} = W_{s, \text{multi-cyl}} = \int_0^{4\pi} M_{s, \text{multi-cyl}}(\theta) d\theta = imep \cdot iV_d = 1398.4 \text{ J} \quad (1.35)$$

$$M_{r, \text{multi-cyl}} = \frac{imep \cdot i \cdot V_d}{4\pi} = 111.28 \text{ Nm} \quad (1.36)$$

$$p_{r, \text{multi-cyl}} = \frac{M_{r, \text{multi-cyl}}}{\frac{V_d}{2}} = 7.16 \text{ bar} \quad (1.37)$$

As for the single-cylinder case, it is also possible to calculate the shaft and the resistant works in the multi-cylinder engine by integrating the shaft and the resistant torque. Normalizing the work terms with respect to the unitary displacement, it is possible to represent the two "pressure terms" and the two "work terms" in the same graph. In this case the period is equal to the phase shift, therefore the plot may be reported only for $0 < \theta < \Delta\varphi$.

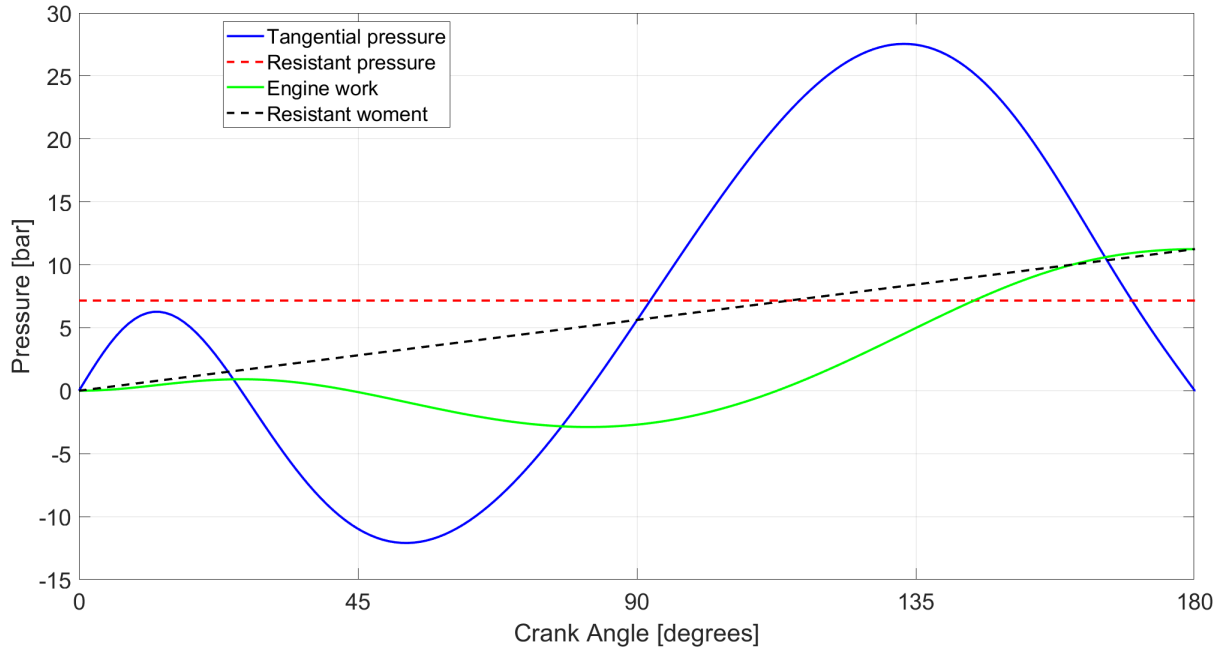


Figure 1.11: Normalized shaft and resistant work over a cycle + tangential and resistant pressure

1.5.2 Calculation of the flywheel diameter

As for the single-cylinder case, it is possible to define the dynamic irregularity:

$$\xi_{multi-cyl} = \frac{\Delta W_{max, multi-cyl} + |\Delta W_{min, multi-cyl}|}{W_{multi-cyl}(4\pi)}$$

$$\Rightarrow \xi_{multi-cyl} = \frac{\Delta W_{tot, multi-cyl}}{imep \cdot iV} = 0.1925 \quad (1.38)$$

Comparing the definition of the dynamic irregularity for the single-cylinder and for the multi-cylinder engine, it would seem logical to expect that the value obtained for the multi-cylinder case is equal to the value obtained for the single-cylinder, divided by the number of cylinders. Anyway, comparing the results:

$$\xi_{multi-cyl} < \frac{\xi_{single-cyl}}{i} \iff 0.1925 < \frac{1.0735}{4}$$

This is due to the fact that the engine torque for a multi-cylinder engine is more regular with respect to the previous case, therefore the quantity of energy "stored" during an engine cycle (normalized over the considered displacement) is lower for the multi-cylinder case. The flywheel inertia required to satisfy the design requirements (kinematic irregularity) can be computed.

$$J_{multi-cyl} = \frac{\xi_{multi-cyl} \cdot imep \cdot V_d}{\delta \cdot \omega_{avg}^2} = 0.0682 \text{ kg} \cdot \text{m}^2$$

$$J_{flyw,multi-cyl} = J_{multi-cyl} - J_{eng} \cdot i = 0.0678 \text{ kg} \cdot \text{m}^2 \quad (1.39)$$

As previously shown for the single cylinder engine with equation 1.28, the flywheel diameter is directly related to the flywheel inertia taking into account the constraints already mentioned about the width.

$$D_{multi-cyl} = \sqrt[5]{\frac{320 \cdot J_{flyw,multi-cyl}}{\rho \cdot \pi}} = 0.2458 \text{ m}$$

It is possible to notice that for our calculation the condition $2S < D < 5S$ has been respected ($2S = 0.1579 \text{ m}$ and $5S = 0.3947 \text{ m}$) so there is no need to change the geometry. As it was previously stated: $w_{flyw,multi-cyl} = \frac{1}{10}D = 0.0246 \text{ m}$

1.5.3 Instantaneous crankshaft speed

The crankshaft instantaneous speed can be calculated applying the same procedure used for the single cylinder case, considering in this case the shaft and resistant work due to all the cylinders. Also in this case the evaluation may be performed over a crank angle interval from 0 to $\Delta\varphi$.

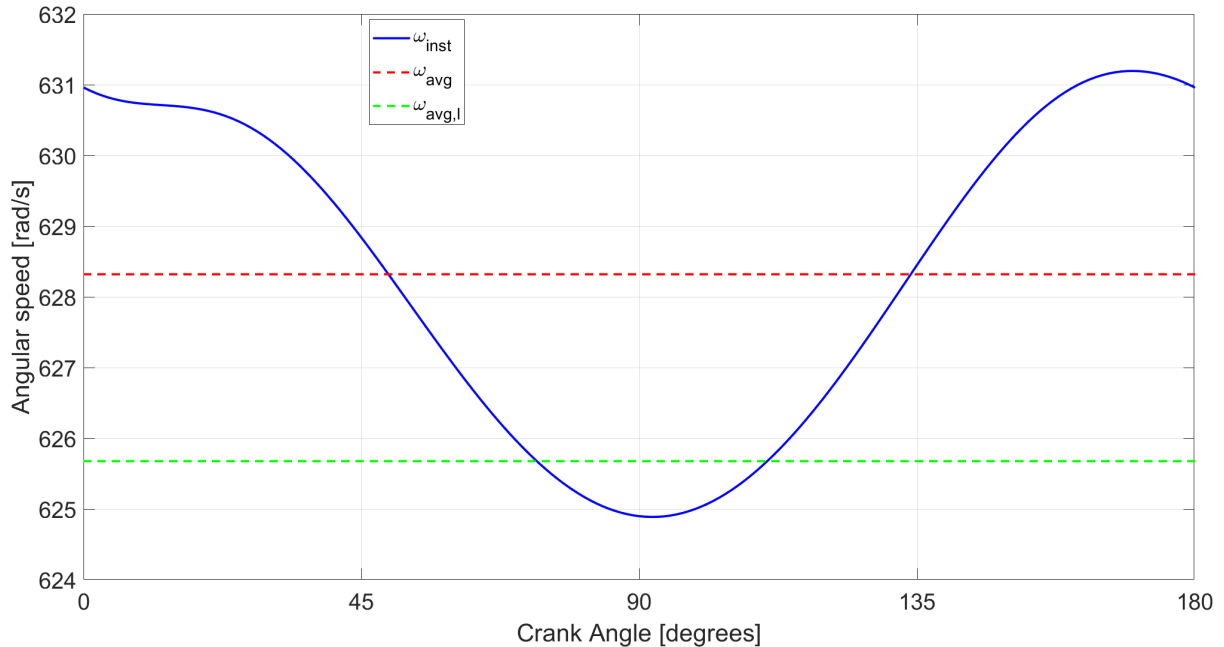


Figure 1.12: Instantaneous crankshaft speed for multi cylinder engine

Report 2

Engine testing and HRR analysis

2.1 Engine testing

A turbocharged CI engine (endowed with EGR) is taken into account for our testing.

Parameter	Value	Unit
Number of cylinders (i)	4	-
Bore (B)	70.8	mm
Stroke (S)	104	mm
Compression ratio (r_c)	17.5	-
Length of connecting rod (l)	158	mm
Displacement volume (V_d)	0.7496	Liters

Table 2.1: Engine characteristics

An engine testbed (figure 2.1) is a complex facility needed to test the engine; the testing is required to characterize the effect of design and calibration parameters on performance and emissions. The testbed has to be designed in order to allow engine operation in every possible working point, being relatable with real working conditions.

Some sensor and a dynamometer (to counteract and measure the engine torque) are needed. A control unit with a user interface is also present: it allows the operator to monitor and control the engine.

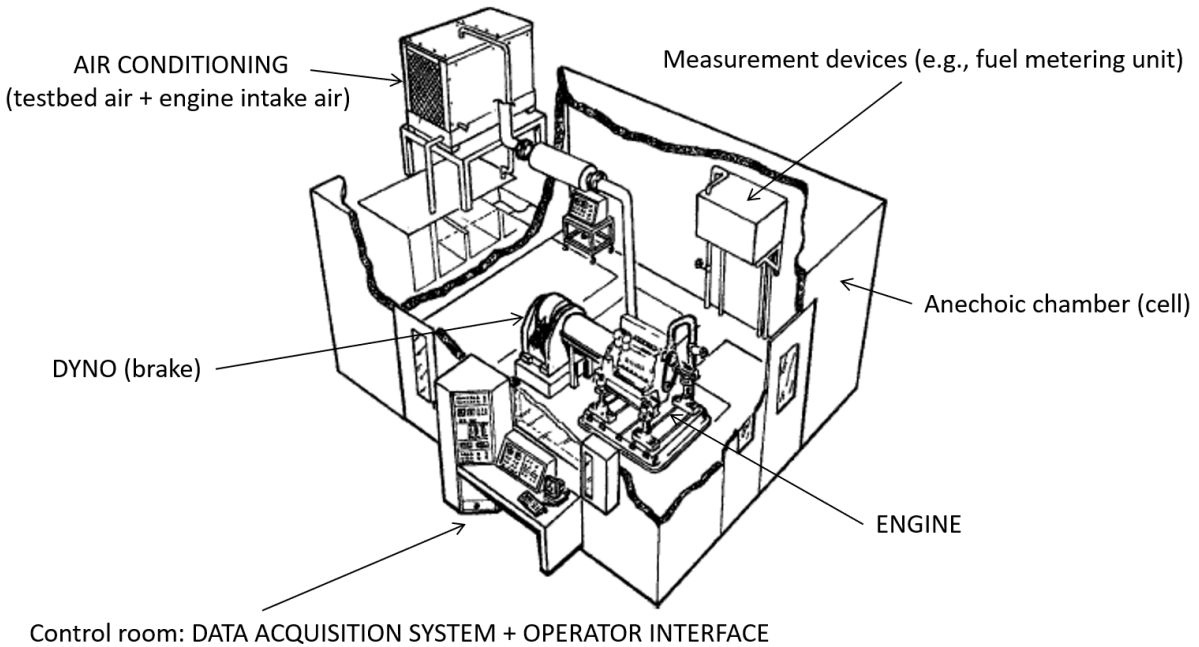


Figure 2.1: Engine testbed

Parameter	Value	Unit
Reference temperature (T_0)	298	K
Reference pressure ($p_{0, dry}$)	99	kPa
Air elastic constant (R)	287.05	$J/(kg \cdot K)$
Lower heating value for the fuel (Q_{LHV})	42.5	MJ/kg
Fuel elastic constant (R)	417	$J/(kg \cdot K)$
EGR specific heat (c_p)	1038	$J/(kg \cdot K)$
EGR elastic constant (R)	296.57	$J/(kg \cdot K)$

Table 2.2: Reference conditions and properties of air, fuel and EGR

2.1.1 Steady state test

Some variables have been measured (and provided as input data) during a set of steady-state tests with different engine speed.

n [rpm]	T_{dyno} [Nm]	\dot{m}_{fuel} [kg/h]	\dot{m}_{air} [kg/h]	\dot{m}_{EGR} [kg/h]
850	233.25	4.701	86.35	0.65
1000	253.25	5.757	108.71	0.70
1200	351.21	9.509	159.74	0.61
1400	421.82	12.81	212.02	3.36
1600	429.50	14.762	247.39	16.52
1800	431.95	16.577	280.07	26.19
2000	433.08	18.468	316.73	33.95
2250	435.44	21.081	370.86	38.72
2500	429.94	23.449	428.87	40.66
2750	426.85	26.217	495.21	45.19
3000	402.56	27.318	537.29	41.26
3250	364.96	27.357	561.97	42.15
3500	339.77	28.006	585.47	39.51
3850	221.99	21.508	532.16	5.33

Table 2.3: Test results

n [rpm]	T_{dyno} [Nm]	p_a [mbar]	T_a [°C]	H_{rel} [%]	T_{im} [°C]	p_{im} [mbar]
850	233.25	1009.91	25.2	48.82	31.0	139
1000	253.25	1009.96	25.1	48.82	30.7	209
1200	351.21	1010.47	25.0	45.27	28.3	505
1400	421.82	1010.45	25.0	45.27	29.8	826
1600	429.50	1010.20	25.3	49.83	35.0	991
1800	431.95	1010.03	25.3	49.83	40.0	1099
2000	433.08	1009.93	25.3	49.54	45.5	1192
2250	435.44	1009.31	25.4	49.54	49.6	1286
2500	429.94	1009.46	25.4	43.53	53.6	1344
2750	426.85	1008.71	25.4	50.28	49.7	1380
3000	402.56	1008.71	25.4	50.34	52.0	1316
3250	364.96	1008.84	25.2	50.28	45.2	1316
3500	339.77	1008.84	25.2	50.28	45.8	1267
3850	221.99	1008.87	25.1	50.17	41.2	864

Table 2.4: Test results

The values of torque and power provided from the testbed need to be corrected by means of a factor μ_C according to ISO1585.

$$\begin{cases} P_0 = \mu_c \cdot P \\ T_0 = \mu_c \cdot T \end{cases} \quad (2.1)$$

For a CI engine, μ_C depends on two dimensionless coefficients:

$$\mu_c = f_a^{f_m} \quad (2.2)$$

According to ISO1585, for a turbocharged CI it is possible to define the first coefficient f_a as it follows:

$$f_a = \left(\frac{p_{0,dry}}{p_{a,dry}} \right)^{0.7} \cdot \left(\frac{T_a}{T_0} \right)^{1.2} \quad (2.3)$$

where T_0 and $p_{0,dry}$ are constant and $p_{a,dry}$ is computed through the following relations:

$$p_{sat,H_20} = a_0 + a_1 T_a + a_2 T_a^2 + a_3 T_a^3 + a_4 T_a^4 \quad (2.4)$$

Where a_0, a_1, \dots, a_4 are coefficients experimentally evaluated.

$$p_{a,dry} = p_a - \mathcal{H}_{rel} \cdot p_{sat,H_20} \quad (2.5)$$

The second coefficient f_m is a function of the corrected fuel delivery parameter q_c

$$q_f = \frac{\dot{m}_f \cdot \frac{1}{60} \cdot 10^6}{\frac{n}{m} \cdot i \cdot V_d} \quad (2.6)$$

$$q_c = \frac{q_f}{\frac{p_{manifold}}{p_a}} \quad (2.7)$$

$$\begin{cases} f_m = 0.036 q_c - 1.14 & \text{if } 37.2 \frac{mg}{l \cdot cycle} \leq q_c \leq 65 \frac{mg}{l \cdot cycle} \\ f_m = 0.2 & \text{if } q_c < 37.2 \frac{mg}{l \cdot cycle} \\ f_m = 1.2 & \text{if } q_c > 65 \frac{mg}{l \cdot cycle} \end{cases} \quad (2.8)$$

n [rpm]	p_{sat, H_2O} [kPa]	$p_{a, dry}$ [kPa]	f_a [-]	q_f [mg/(l · cycle)]	q_c [mg/(l · cycle)]	f_m [-]	μ_c [-]
850	3.2065	99.4257	0.9978	61.480	54.037	0.8053	0.9987
1000	3.1875	99.4399	0.9973	63.997	53.007	0.7683	0.9979
1200	3.2642	99.4788	0.9986	88.088	58.754	0.9751	0.9982
1400	3.1856	99.6109	0.9957	101.175	55.997	0.8750	0.9980
1600	3.2256	99.4127	0.9983	102.563	51.771	0.7273	0.9982
1800	3.2449	99.4104	0.9987	102.376	49.078	0.6268	0.9983
2000	3.2256	99.3248	0.9989	102.649	47.057	0.5540	0.9984
2250	3.2049	99.3234	0.9993	104.135	45.807	0.4915	0.9985
2500	3.1685	99.4986	0.9965	104.267	44.708	0.4695	0.9984
2750	3.2449	99.2397	0.9999	105.978	44.509	0.4623	1.0000
3000	3.2449	99.2286	1.0000	101.226	42.741	0.3987	1.0000
3250	3.2065	99.2029	0.9999	93.575	40.061	0.3216	0.9999
3500	3.2065	99.2582	0.9990	89.436	39.425	0.2793	0.9999
3850	3.1875	99.2877	0.9984	62.102	33.451	0.2000	0.9997

Table 2.5: ISO1585 Calculations

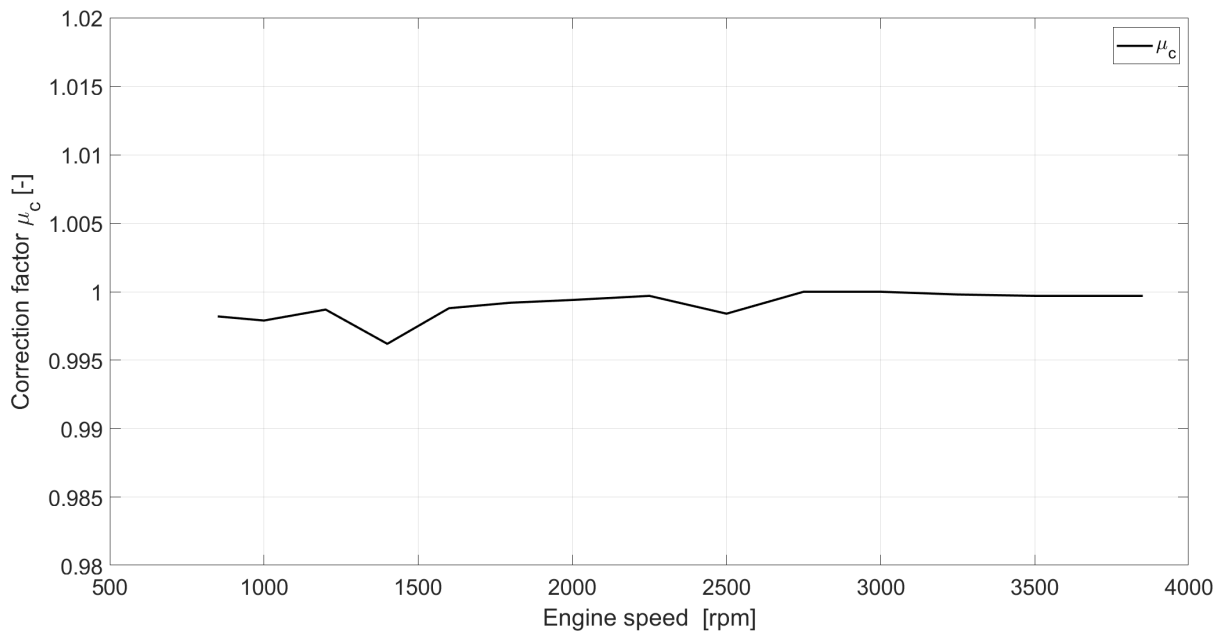


Figure 2.2: Correction factor

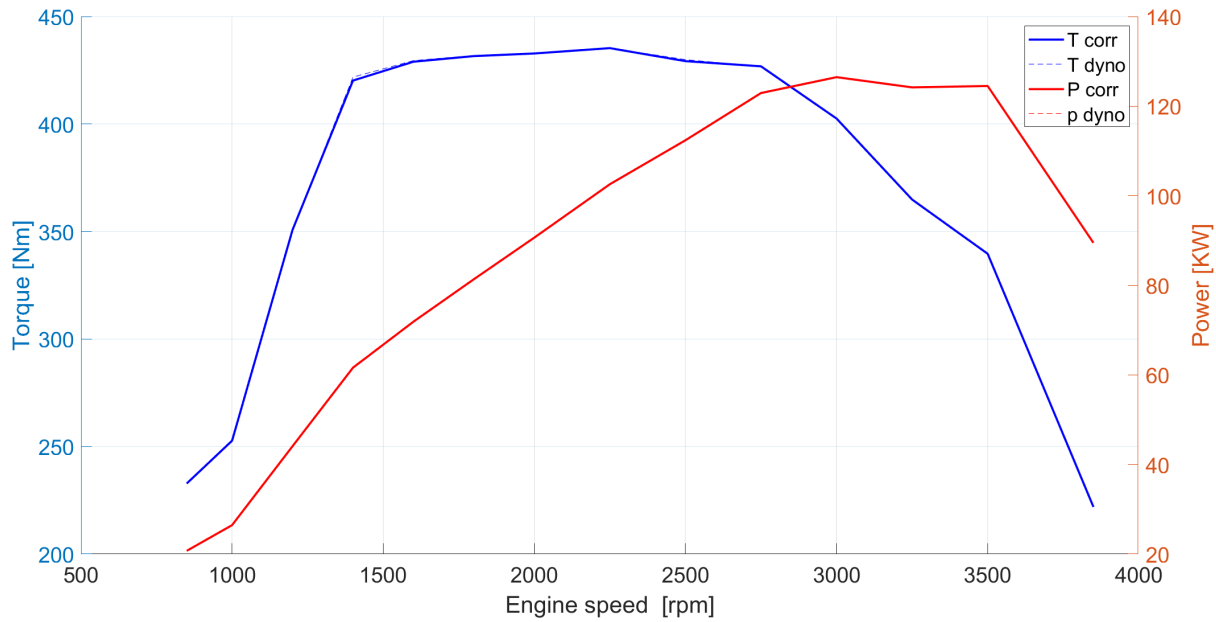


Figure 2.3: Mechanical characteristic

Since $0.995 < \mu_C < 1$, it is possible to observe that the corrected characteristics differ from the uncorrected one due to extremely tiny quantities: the plotted quantities of the corrected characteristics overlap the uncorrected ones.

Additionally, the corrected power P can be used to compute the brake specific fuel consumption and fuel conversion efficiency:

$$bsfc = \frac{\dot{m}_f}{P} \quad (2.9)$$

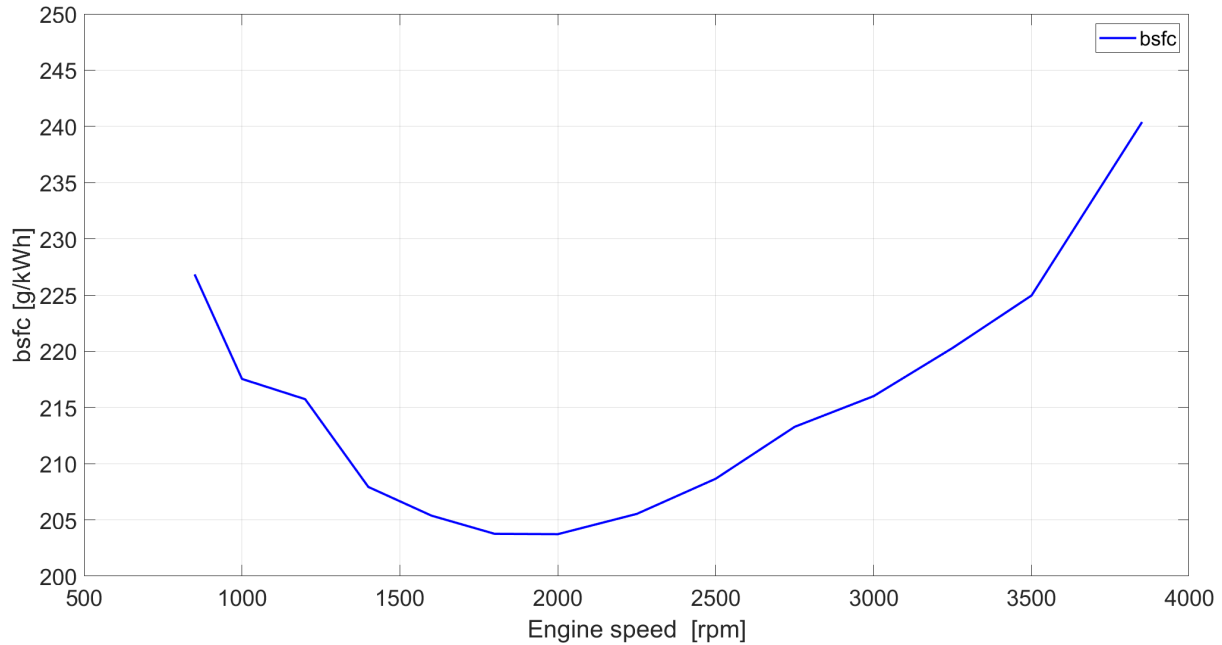


Figure 2.4: Brake specific fuel consumption

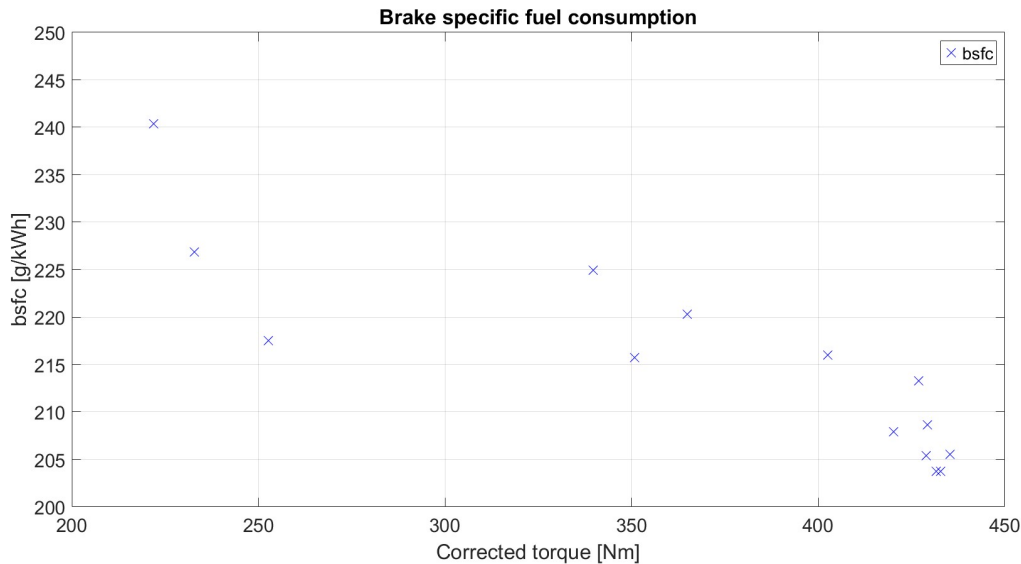


Figure 2.5: Brake specific fuel consumption

$$\eta_f = \frac{P}{\dot{m}_f \cdot Q_{LHV}} \quad (2.10)$$

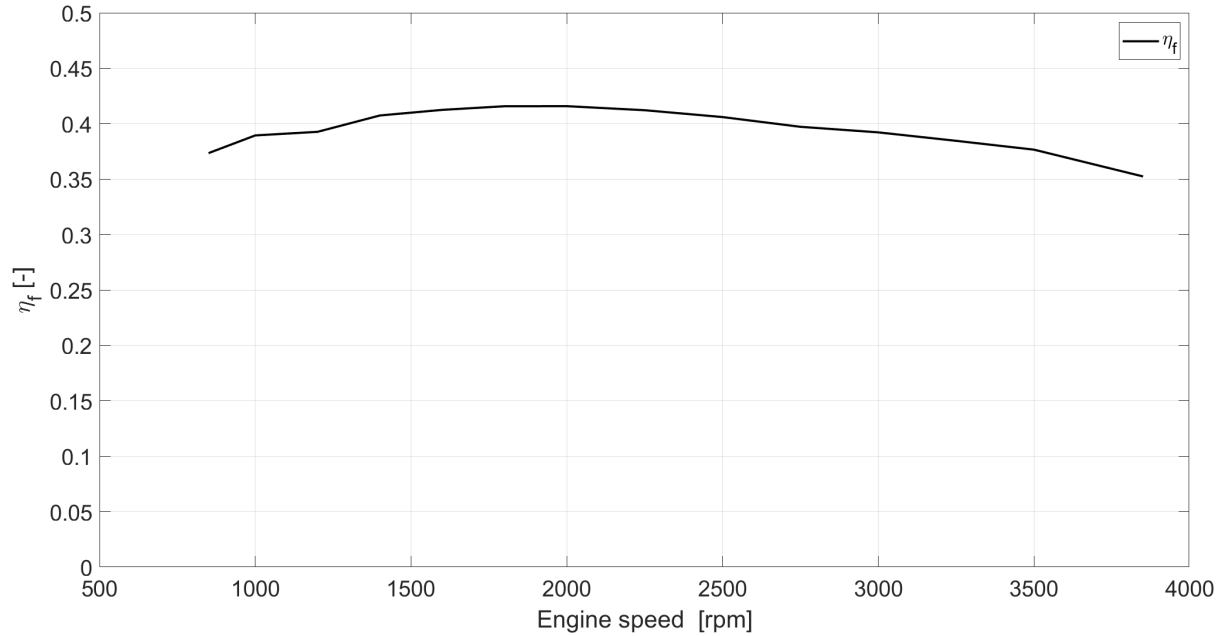


Figure 2.6: Fuel conversion efficiency

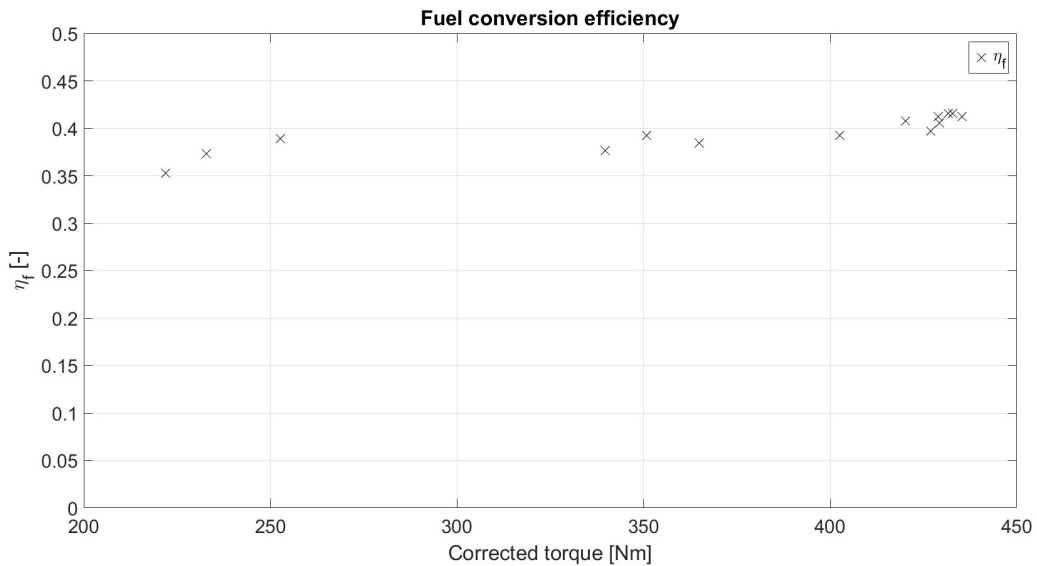


Figure 2.7: Fuel conversion efficiency

The volumetric efficiency can be computed as it follows:

$$\lambda_v = \frac{m_{\text{int}}}{m_{\text{int,ref}}} = \frac{m_a + m_{\text{EGR}}}{\rho_{\text{int}} V_d} = \frac{m_a + m_{\text{EGR}}}{V_d} \cdot \frac{R_{\text{mix}} \cdot T_{\text{int}}}{p_{\text{int}}} \quad (2.11)$$

where:

$$R_{\text{mix}} = \frac{\dot{m}_{\text{air}} R_{\text{air}} + \dot{m}_{\text{EGR}} R_{\text{EGR}}}{\dot{m}_{\text{air}} + \dot{m}_{\text{EGR}}} \quad (2.12)$$

n [rpm]	R_{mix} [J/(kg · K)]	λ_v [-]
850	287.12	0.8843
1000	287.28	0.8863
1200	287.09	0.8476
1400	287.20	0.8085
1600	287.65	0.8119
1800	287.87	0.8093
2000	287.97	0.8120
2250	287.95	0.8196
2500	287.87	0.8343
2750	287.55	0.8158
3000	287.33	0.7961
3250	287.26	0.7724
3500	287.15	0.7611
3850	287.14	0.7475

Table 2.6: Volumetric efficiency

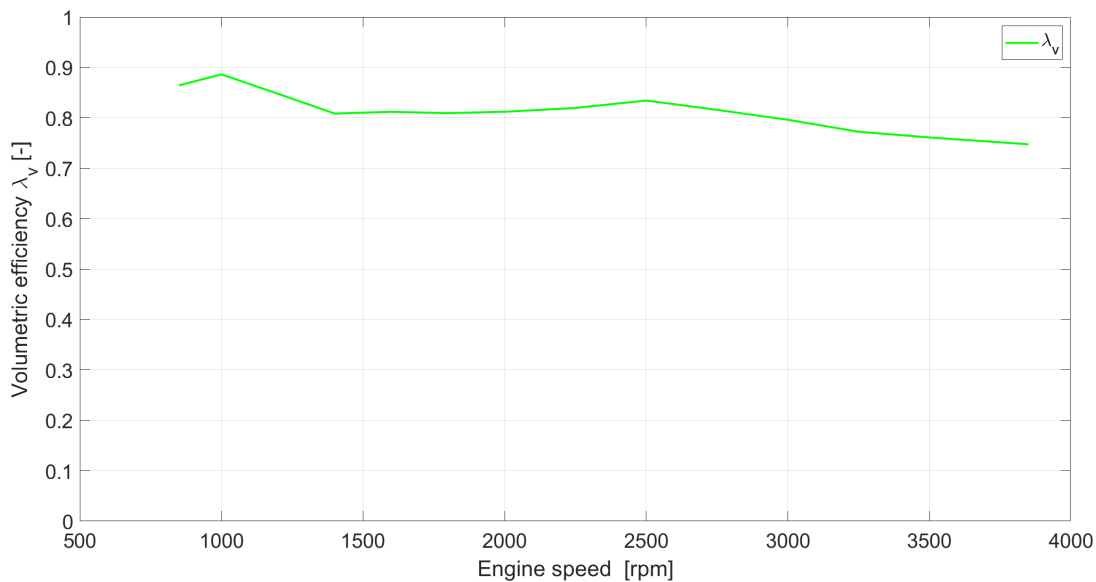


Figure 2.8: Volumetric efficiency

2.2 HRR analysis

An heat releasing rate analysis based on a single-zone model (uniform average T related to both burned/unburned gas) is performed, considering 100 in-cylinder cycles (for each cylinder) with 7200 pressure measurements provided.

2.2.1 Evaluation and filtering of in-cylinder pressure signal

Since a **piezoelectric transducer** is not able to provide an absolute pressure (it only provides the shape of the variation relative to the previous instant), a proper pegging pressure is going to be considered in order to compute the absolute in-cylinder pressure. Actually, the pegged measurements are provided from a **piezoresistive transducer**.

In order to get a proper pegging, the mean pressure on an angular interval of $10^\circ CA$ (from 175° to 185°) is used to evaluate the shift. Once the shift is applied to each cycle (which means the 100 cycles are pegged) the average cycle can be evaluated:

MATLAB script - Trasductor analysis

```

1 load("ifile_2000FL.mat")
2 file_name = 'datasheet';
3 HRR_data_add = xlsread(file_name, 'HRR point', 'B:B');
4 S = double(ifile.engine.stroke); % stroke [mm]
5 p_raw = double(ifile.PCYL1.data); %100 cycles, each of them with
   ↳ 7200 pressure values [bar]
6 p_man = double(ifile.PMAN1.data);
7 p_raw_peg = zeros(7200,100);
8 for i = 1:100 %pegging
9     p_raw_i = p_raw(:,i);
10    p_man_i = p_man(:,i);
11    p_cyl1_avg = mean(p_raw_i(1750:1850)); %piezoelectric
      ↳ trasductor
12    p_man_avg = mean(p_man_i); %piezoresistive trasuctor
13    shift = p_man_avg-p_cyl1_avg;
14    p_raw_peg(:,i) = p_raw_i + shift;
15 end
16 p_raw_mean = mean(p_raw_peg, 2); %average cycle of the 100 once
   ↳ they are pegged

```

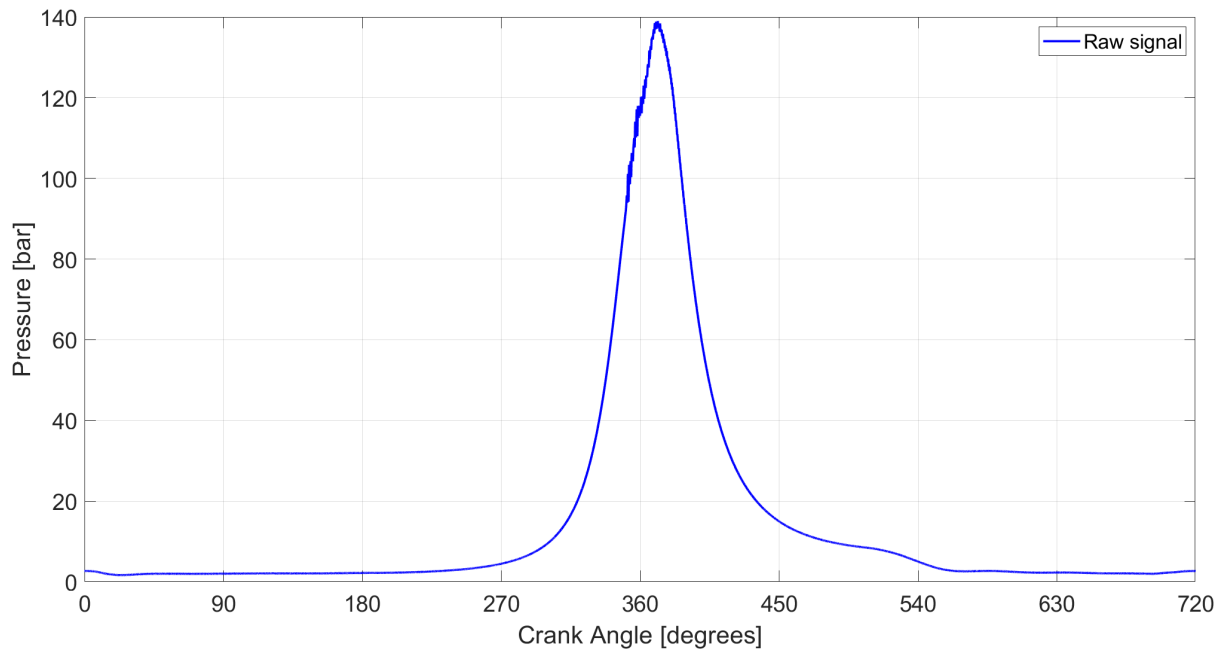


Figure 2.9: Average cycle as a pressure raw signal

In order to have a smooth function the *Butterworth filter* has been chosen. This is a low-pass filter in which high frequencies are damped. The following MATLAB script has been used.

MATLAB script - Butterworth filter

```

1 fs = 2000/60*360/0.1; %sampling frequency
2 fc = 4000; %cutoff frequency [Hz]
3 Wn = fc/(fs/2); %ratio between cutoff and Nyquist frequency
4 n = 2; % order of the filter
5 [b,a] = butter(n,Wn);
6 p_cyl_butter_filtfilt=filtfilt(b,a,p_raw_mean);
7 p_cyl_butter_filt=filter(b,a,p_raw_mean);

```

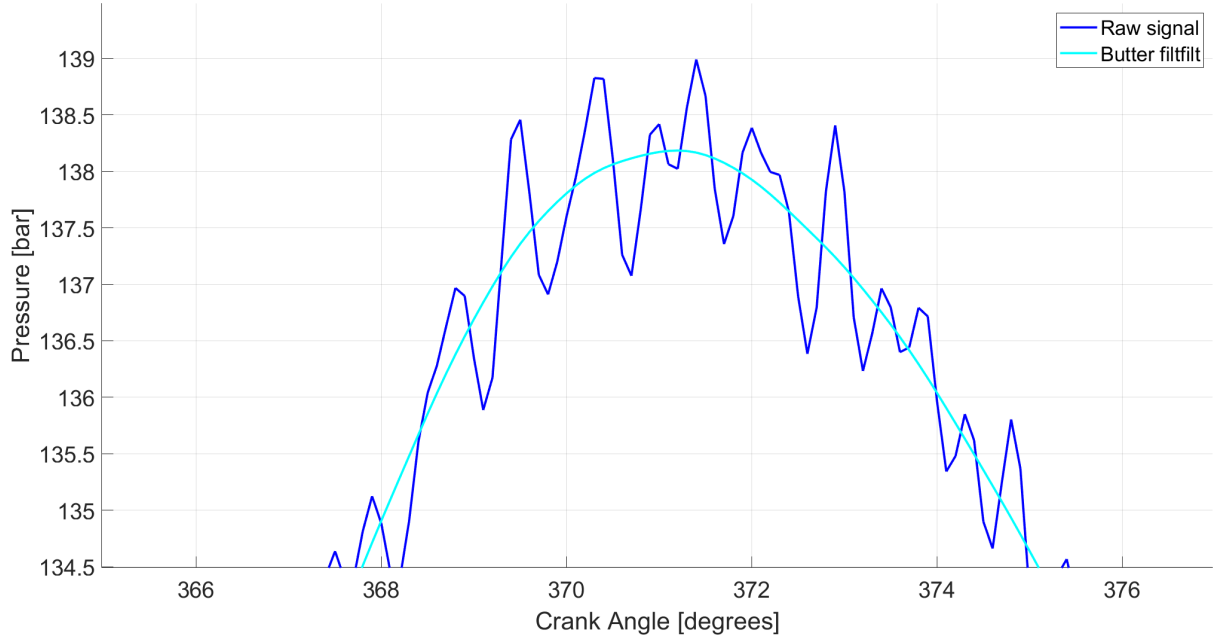


Figure 2.10: Signal comparison after filtering

2.2.2 Combustion diagnostic and mass fraction burned calculations

Through this approach it is possible to account for the effect of heat transfer and leakages by applying the first principle of thermodynamics to the content of the combustion chamber. The basic hypothesis (behind the single-zone model) is that the gas inside the chamber can be considered homogeneous. By studying the “average” thermodynamic state of the cylinder charge starting from the measured pressure and volume change, it is possible to determine the net heat release rate (also named apparent HRR).

$$\dot{Q}_n = \dot{Q}_{ch} - \dot{Q}_{ht} = \dot{W} + \frac{dU_{th}}{dt} + \sum h_i \cdot m_i \quad (2.13)$$

$$dQ_n = \frac{\gamma}{\gamma - 1} \cdot p dV + \frac{1}{\gamma - 1} \cdot V dp \quad (2.14)$$

$$HRR = \frac{dQ_n}{d\theta} = \frac{\gamma}{\gamma - 1} \cdot p \frac{dV}{d\theta} + \frac{1}{\gamma - 1} \cdot V \frac{dp}{d\theta} \quad (2.15)$$

It must be considered that the isentropic coefficient used in the previous relations changes with temperature according to the following empirical relation:

$$\gamma = 1.338 - 6 \cdot 10^{-5} \cdot T + 1 \cdot 10^{-8} \cdot T^2 \quad (2.16)$$

where:

$$T = \frac{pV}{m_{mix} \cdot R_{mix}} \quad (2.17)$$

In addition, it could be helpful to understand how the in-cylinder pressure measurements (raw and filtered ones) differs from the motored pressure. It can now be computed since the isentropic coefficient is evaluated for all the points of the cycle, knowing that for a motored cycle $pV^\gamma = \text{const}$

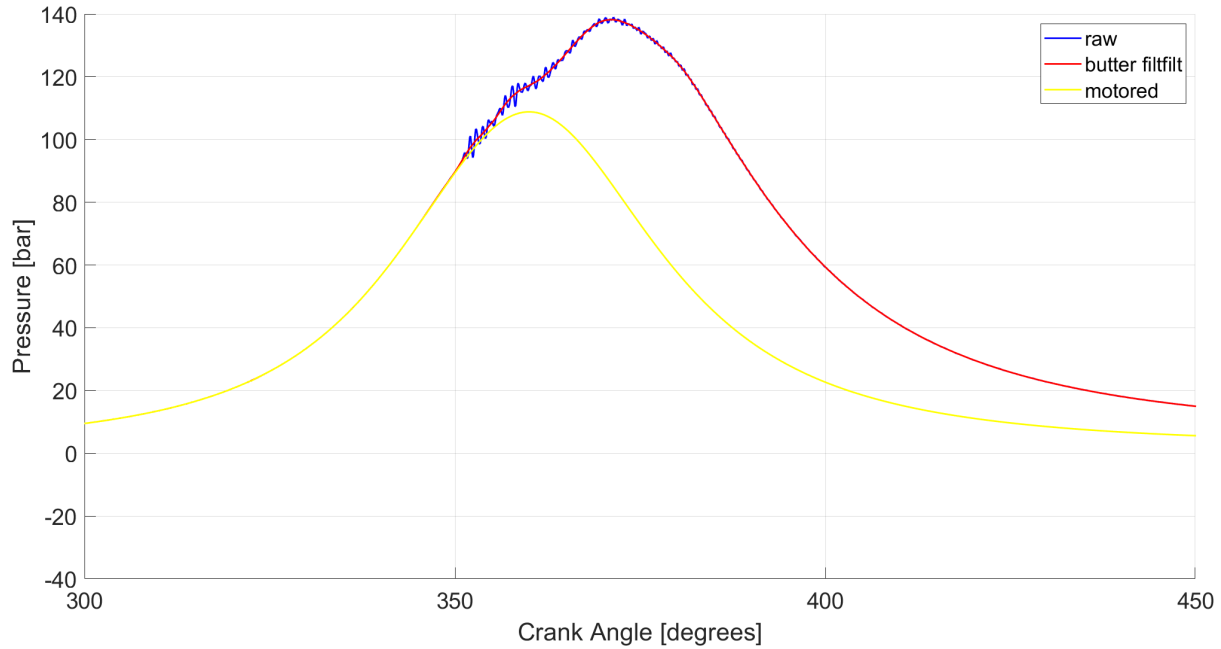


Figure 2.11: Comparison of cycles

From the heat release analysis:

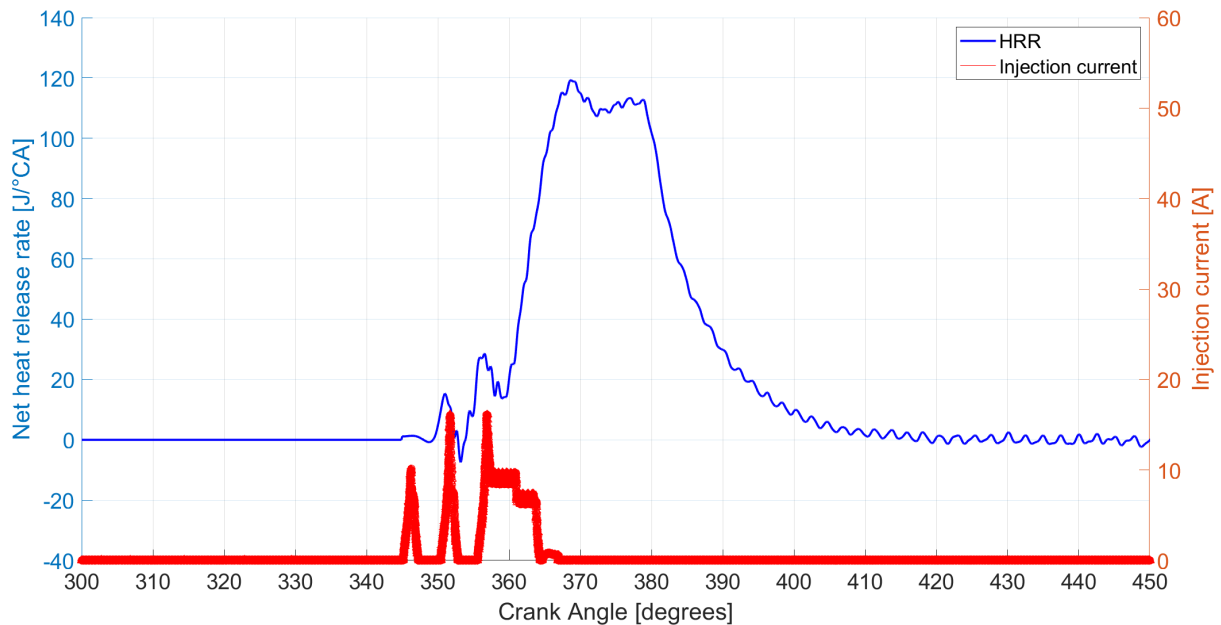


Figure 2.12: HRR and injection current

The start of injection SOI can be evaluated from the input data of the electrical signal from injectors, seeing where the electrical current to the injectors starts to increase.

$$SOI = 345^\circ$$

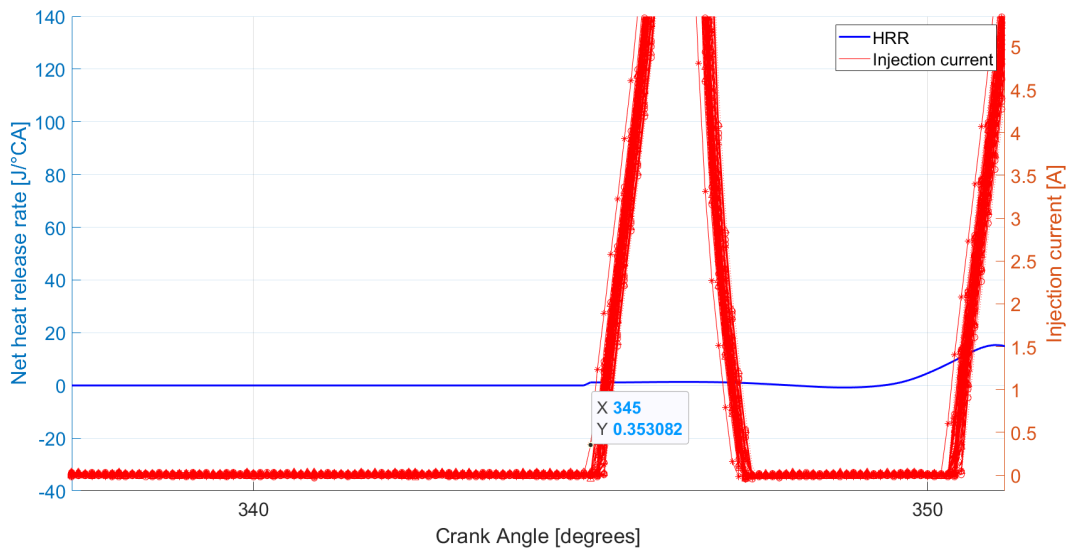


Figure 2.13: SOI from injection current signal

The start of combustion can be estimated from the HRR curve when the signal is crossing zero after the first minimum.

$$SOC = 349.4^\circ$$

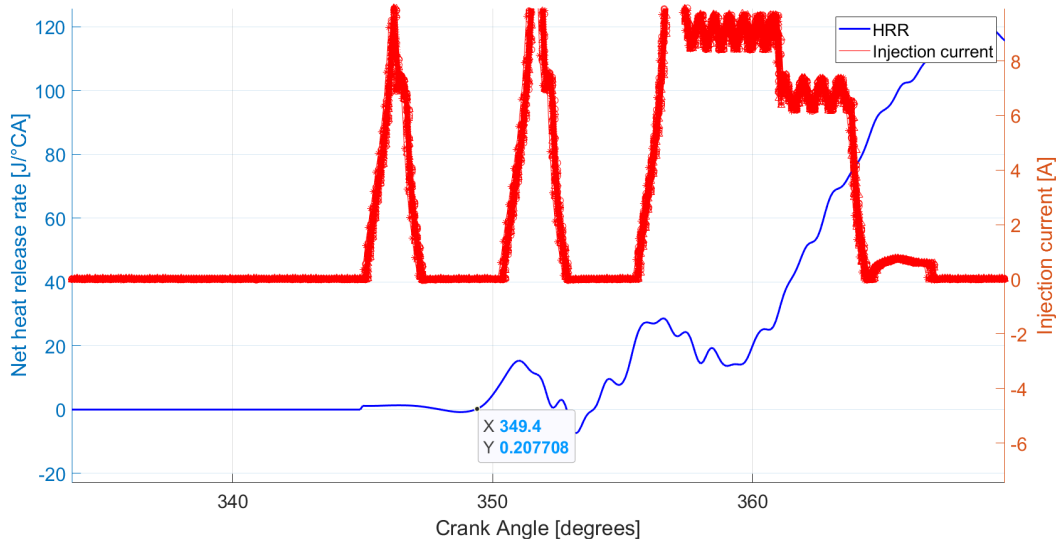


Figure 2.14: SOC from Heat Release Rate

The ignition delay, which is the angular interval needed to atomize, vaporize and mix the fuel prior to ignition, can be estimated as:

$$ID = SOC - SOI = 4.4^\circ$$

The mass fraction burned can be estimated as it follows:

$$x_b(\theta) = \frac{\int_{SOI}^{EOC} HRR \cdot d\theta}{m_{f,inj,TOT} \cdot Q_{LHV}} \quad (2.18)$$

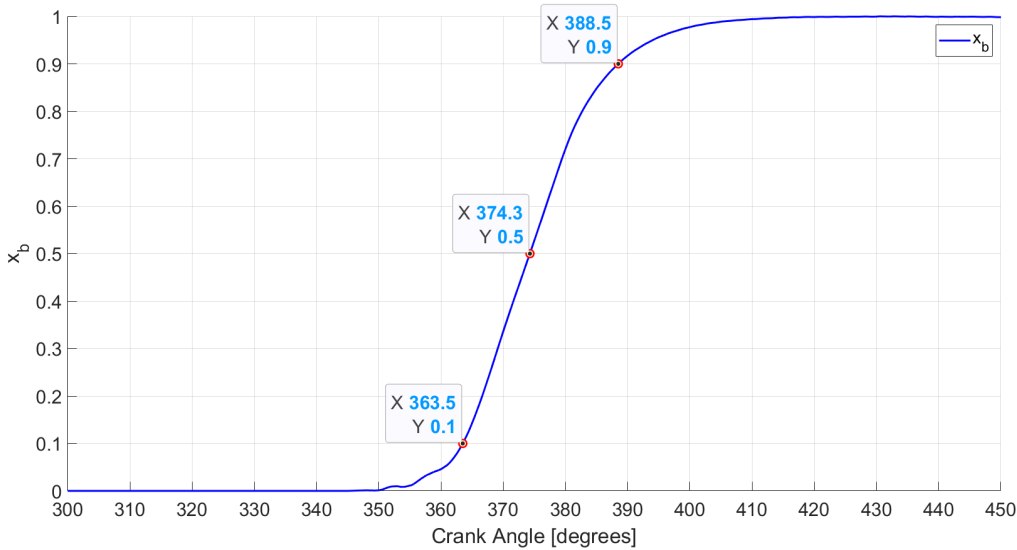


Figure 2.15: Mass fraction burned

The values of MFB10, MFB50 and MFB90 can be extracted from previous plot, respectively looking where the function reaches the values of 0.1, 0.5 and 0.9.

$$MFB10 = 363.5^\circ$$

$$MFB50 = 374.3^\circ$$

$$MFB90 = 388.5^\circ$$